THE JOURNAL OF BIOLOGICAL CHEMISTRY VOL. 290, NO. 15, pp. 9412–9427, April 10, 2015

Parkinson Disease Mutant E46K Enhances α-Synuclein Phosphorylation in Mammalian Cell Lines, in Yeast, and *in Vivo*[*]

Received for publication, October 18, 2014, and in revised form, January 30, 2015 Published, JBC Papers in Press, February 5, 2015, DOI 10.1074/jbc.M114.610774

Martial Kamdem Mbefo[‡], Mohamed-Bilal Fares[‡], Katerina Paleologou[‡], Abid Oueslati[‡], Guowei Yin[§], Sandra Tenreiro[¶], Madalena Pinto[¶], Tiago Outeiro[¶‖1], Markus Zweckstetter[§‡‡], Eliezer Masliah[§§], and Hilal A. Lashuel[‡2]**

*From the [‡]Laboratory of Molecular and Chemical Biology of Neurodegeneration, Brain Mind Institute, Ecole Polytechnique Federale de Lausanne, Station 15, 1015 Lausanne, Switzerland, the [§]Department of NMR-based Structural Biology, Max Planck Institute for Biophysical Chemistry, Am Fassberg 11, 37077 Göttingen, Germany, the [¶]Cell and Molecular Neuroscience Unit, Instituto de Medicina Molecular, and [‖]Instituto de Fisiologia, Faculdade de Medicina, Universidade de Lisboa, Av. Prof. Egas Moniz 1649-028 Lisboa, Portugal, the **Department of NeuroDegeneration and Restorative Research, University Medical Center Goettingen and the [‡‡]German Center for Neurodegenerative Diseases, Am Fassberg 11, 37077 Göttingen, Germany, and the [§§]Departments of Pathology and Neurosciences, School of Medicine, University of California at San Diego, San Diego, California 92103*

Background: Little is known about the effect of PD-linked mutations on α-synuclein (α-syn) phosphorylation.
Results: The E46K mutation increases α-syn phosphorylation at Ser-129 and influences its subcellular localization *in vivo*.
Conclusion: The E46K mutation alters α-syn localization and post-translational modifications.
Significance: PD-linked α-syn mutations may contribute to PD via different mechanisms.

Although α-synuclein (α-syn) phosphorylation has been considered as a hallmark of sporadic and familial Parkinson disease (PD), little is known about the effect of PD-linked mutations on α-syn phosphorylation. In this study, we investigated the effects of the A30P, E46K, and A53T PD-linked mutations on α-syn phosphorylation at residues Ser-87 and Ser-129. Although the A30P and A53T mutants slightly affected Ser(P)-129 levels compared with WT α-syn, the E46K mutation significantly enhanced Ser-129 phosphorylation in yeast and mammalian cell lines. This effect was not due to the E46K mutant being a better kinase substrate nor due to alterations in endogenous kinase levels, but was mostly linked with enhanced nuclear and endoplasmic reticulum accumulation. Importantly, lentivirus-mediated overexpression in mice also showed enhanced Ser-129 phosphorylation of the E46K mutant compared to WT α-syn, thus providing *in vivo* validation of our findings. Altogether, our findings suggest that the different PD-linked mutations may contribute to PD pathogenesis via different mechanisms.

Parkinson disease (PD)[3] is a neurodegenerative movement disorder characterized by the loss of dopamine-producing neurons in the substantia nigra (1). The main histopathological feature of PD is the formation of intracellular inclusions called Lewy bodies (LBs) that form as a result of the fibrillization of the presynaptic protein α-synuclein (α-syn). Several point mutations in the gene coding for α-syn (*SNCA*) were identified and linked to the autosomal dominant inherited form of PD as follows: A53T (2–4), A30P (5), E46K (6), and recently H50Q (7, 8), G51D (9), and A53E (10). Therefore, a better understanding of the mechanisms by which these mutations alter the physiological and pathogenic properties of α-syn could provide critical insights into the molecular basis underlying the pathogenesis of PD, and aid in the development of strategies to treat or prevent the disease.

α-syn belongs to a class of natively unfolded proteins and adopts an ensemble of disordered conformations in solution (11, 12). However, at neutral pH, long range transient intramolecular interactions between the C- and N-terminal regions of the protein have been observed by NMR (13) and can be stabilized by chemical cross-linking (14). α-syn readily adopts an α-helical structure upon interaction with small unilamellar vesicles and micelles containing negatively charged lipids and detergents (15), supporting its association with presynaptic vesicles *in vivo*, and consistent with its localization to axonal termini (16–18). The interactions of α-syn with membranes are mediated by its N terminus (residues 1–60), which encompasses the PD-linked mutations, and also by the nonamyloid component region comprising residues 61–95 (19, 20). Notably, whereas the A30P and G51D mutants exhibit defective interaction with membranes (21–25), the E46K mutation increases the binding affinity of α-syn to phospholipids (21, 26), probably due to the formation of an additional hydrogen bond between the extra lysine

* This work was supported in part by Ecole Polytechnique Fédérale de Lausanne, Swiss National Science Foundation Grant 31003A_120653, the Michael J. Fox Foundation, Merck Serono, a Marie Curie post-doctoral fellowship (to A. O.), the Cluster of Excellence and Deutsche Forschungsgemeinschaft Research Center "Nanoscale Microscopy and Molecular Physiology of the Brain" (to M. Z.), Fundação para a Ciência e Tecnologia Projects PTDC/SAU-NEU/105215/2008 and PTDC/BIA-BCM/117975/2010, and Post-doctoral Fellowships SFRH/BPD/35767/2007 (to S. T.) and IMM/BTI/1-2012 (to M. R. P.).
[1] Supported by an EMBO Installation Grant.
[2] To whom correspondence should be addressed: Laboratory of Molecular and Chemical Biology of Neurodegeneration, Brain Mind Institute, Ecole Polytechnique Federale de Lausanne, CH-1015 Lausanne, Switzerland. Tel.: 41-21-693-96-91; Fax: 41-21-693-17-80; E-mail: hilal.lashuel@epfl.ch.
[3] The abbreviations used are: PD, Parkinson disease; α-syn, α-synuclein; CK1, casein kinase 1; CK2, casein kinase 2; GRK, G protein-coupled receptor kinase, PLK, Polo-like kinase; LB, Lewy bodies; ER, endoplasmic reticulum; BisTris, 2-[bis(2-hydroxyethyl)amino]-2-(hydroxymethyl)propane-1,3-diol; HSQC, heteronuclear single quantum coherence; ANOVA, analysis of variance; LV, lentiviral vector.

in the protein and micelles (27). Another important feature of the PD-linked mutations is their differential propensity to aggregate *in vitro*. Although the A53T, E46K, and H50Q mutants enhance α-syn fibrillization (28–34), the A30P mutant exhibits only enhanced oligomerization rate compared with WT α-syn (31, 35, 36), and the G51D and A53E mutations attenuate α-syn fibrillization and favor the formation of amorphous aggregates (25, 37).

In addition to genetic mutations, post-translational modifications, notably phosphorylation, have been reported to dramatically affect α-syn aggregation and toxicity (1). Indeed, α-syn phosphorylation at Ser-129 (Ser(P)-129) has emerged as a pathological hallmark of PD and other synucleinopathies, although the precise effect of this modification on LB formation and α-syn toxicity is not yet completely understood. Interestingly, α-syn isolated from detergent-insoluble fractions of PD brains bearing the A53T mutation was shown to be phosphorylated at Ser-129 (38). Moreover, Ser(P)-129 α-syn-positive inclusions were detected in brains of symptomatic transgenic mice expressing E46K α-syn (39), suggesting that α-syn PD-linked mutations and post-translational modifications could play a synergistic role on α-syn toxicity *in vivo*. However, whether the PD-linked mutations affect α-syn phosphorylation at Ser(P)-129 remains unclear. A previous study showed that A30P and A53T do not influence the effect of phosphorylation on the formation of inclusions (40), whereas a follow-up study by Ishii *et al.* (41) reported that *in vitro* phosphorylation of α-syn by casein kinase 2 (CK2) is slower for A30P and A53T compared with WT α-syn. However, it is noteworthy that CK2 is not an efficient kinase for phosphorylating α-syn *in vitro* (42) and that the effect of the E46K mutant was not investigated in both studies.

To further explore the interplay between α-syn PD-linked mutations and pathological post-translational modifications, we investigated the effects of the A30P, E46K, and A53T mutations on α-syn phosphorylation at Ser-87 and Ser-129 by endogenous kinases in mammalian cell lines and in yeast. Interestingly, whereas Ser(P)-129 levels were reduced in the A30P case, both A53T and E46K mutants consistently exhibited increased Ser(P)-129 phosphorylation levels compared with WT α-syn, with the E46K mutant having the most prominent effect. Importantly, lentivirus-mediated overexpression of E46K α-syn in the hippocampus of mice showed similarly enhanced Ser(P)-129 phosphorylation. Intrigued by this observation, we set to determine whether this effect is due to 1) the E46K mutant being a better kinase substrate *in vitro* and in cells, 2) alterations in endogenous kinase levels, 3) impairment in Ser(P)-129 or total α-syn degradation, or 4) differences in α-syn subcellular localization. Our results show that the enhanced phosphorylation of the E46K mutant could be linked with the aberrant subcellular localization of this mutant. This suggests that the different PD-linked mutations may contribute to the pathogenesis of PD via different mechanisms, and that improper localization of α-syn could alter its phosphorylation state at Ser-129.

EXPERIMENTAL PROCEDURES

Plasmids and Expression and Purification of ^{15}N-Labeled α-syn—The pCDNA6 Human α-syn WT was kindly provided by Prof. Peter T. Lansbury, Jr. (Dept. of Neurology, Harvard Medical School, Cambridge, MA). pCDNA6 human A30P, E46K, and A53T α-syn were obtained by site-directed mutagenesis using the human pCDNA6 α-syn WT plasmid as a template. pAAV human α-syn S129A was obtained by site-directed mutagenesis using the human pAAV CMV α-syn WT (43) as template. The GFP-CL1 construct was kindly provided by Professor Darren Moore (Ecole Polytechnique Federale de Lausanne, Switzerland). All constructs were confirmed by DNA sequencing (Microsynth, Switzerland). Expression and purification of non-labeled as well as ^{15}N-labeled WT and mutant (A30P, E46K, and A53T) α-syn was performed as described previously (42, 44).

Yeast Strains and Plasmids—WT, A30P, E46K, and A53T α-syn cloned into p426GPD (45) were subcloned into the SpeI-HindIII sites of the p426GAL yeast expression vector (46). The GRK2 and GRK5 cDNAs were excised from the mammalian expression vector pRK5 (47) and cloned into the EcoRI and SalI sites of p423GPD. The CK2α cDNA was excised from the yeast expression vector p426TEF (48) and cloned into the SpeI and EcoRI sites of p423GPD. The PLK1 Myc-FLAG cDNA was excised from the mammalian expression vector pCMV6 (43) and cloned into the ClaI and EcoRI sites of p423GAL, whereas PLK2 Myc-FLAG, PLK3 Myc-FLAG, and PLK4 Myc-FLAG were excised from pCMV6 (43) and cloned into the ClaI and BamHI sites of p423GAL. The vector control strain contained the corresponding empty vector (p426GAL and p423GAL). The yeast strain used was BY4147 (*MAT***a**; *his3*Δ*1*; *leu2*Δ*0*; *met15*Δ*0*; *ura3*Δ*0*). Yeast transformations were carried out using a standard lithium acetate protocol. Yeast strains were grown in synthetic complete (SC) medium (6.7 g/liter Yeast Nitrogen Base (BD Biosciences), appropriate amino acid dropout mix (Sunrise Science Products) without the appropriate plasmid selection auxotrophy (uracil or uracil and histidine), and with 1% (w/v) raffinose or 1% (w/v) galactose as carbon source). Yeast strains carrying the galactose-inducible α-syn constructs were pre-grown in raffinose medium (no repression of the galactose-inducible promoter) prior to galactose medium to allow rapid, synchronous induction of expression.

Construction of Lentiviral Vectors—The full-length human α-syn WT and the point mutant E46K cDNA was PCR-amplified and cloned into the third generation self-inactivating lentivirus vector with the CMV promoter driving expression producing the vector LV-α-syn WT and α-syn E46K. The lentiviral vector expressing the human WT α-syn has been previously described (49). Lentiviruses expressing WT and mutant α-syn as well as empty vector (LV-control) were prepared by transient transfection in HEK293T cells as described previously (49). Viral titers were determined by p24 ELISA.

Antibodies—The sheep monoclonal anti-α-syn (catalog no. AB5336P) and mouse monoclonal anti-α-syn SC211 (catalog no. SC-12767, 1:1000) were obtained from Millipore and Santa Cruz Biotechnology, respectively. Monoclonal anti-phosphorylated (Ser(P)-129) α-syn (catalog no. 014-20281, 1:5000) was

obtained from Wako. Mouse monoclonal anti-β-actin (catalog no. Ab6276-100, 1:20000) was from Abcam. The Proteo-Extract® antibody kit (catalog no. 71771-3), containing a mouse monoclonal anti-calnexin antibody, a mouse monoclonal anti-HSP90 antibody, a mouse monoclonal anti-PARP1a antibody, and a mouse monoclonal anti-vimentin antibody, was obtained from Calbiochem. Anti-phospho-Ser-87 (Ser(P)-87) α-Syn antibody was generated in our laboratory (50). The goat polyclonal anti-Ck2α (SC-6479,1:5000) the rabbit polyclonal anti-GRK2 (SC-562, 1:5000), and the rabbit polyclonal anti-GRK5 (SC-565, 1:5000) were obtained from Santa Cruz Biotechnology. The mouse anti-Myc (catalog no. 2276, 1:1000) was obtained from Cell Signaling Technology. The mouse anti-GAPDH (AM4300, 1:5000) was from Ambion.

In Vitro Phosphorylation of ^{15}N-Labeled α-syn—WT or mutant α-syn was phosphorylated by CK1 (1,000,000 units/ml, New England Biolabs) or PLK2 (0.48 mg/ml, Invitrogen). For CK1 real time phosphorylation, the ^{15}N-labeled α-syn was employed at a concentration of 225 μM in a solution containing 1.09 mM ATP and 1× CK1 Reaction Buffer (supplied with the CK1 enzyme), pH 7.4. For PLK2 real time phosphorylation, the ^{15}N-labeled α-syn was employed at a concentration of 100 μM in a solution containing 1.09 mM ATP (freshly prepared), 20 mM HEPES, 10 mM $MgCl_2$, and 2 mM DTT, pH 7.4. The amount of PLK2 used was 0.75 μg for 144 μg of α-syn.

Kinetics of Phosphorylation Assessed by NMR Spectroscopy—NMR data were acquired on Bruker Avance 600 and 700 MHz NMR spectrometers. Tentative assignments for the spectra of mutant and phosphorylated proteins were obtained by transferring each previously assigned cross-peak (13) in the two-dimensional ^{1}H-^{15}N heteronuclear single quantum coherence (HSQC) spectrum of the WT protein to the nearest unassigned cross-peak in each new spectrum. In the case of CK1 phosphorylation, the kinase was incubated at 37 °C for 5 min before mixing it with the protein (225 μM) in CK1 Reaction Buffer (New England Biolabs), pH 7.4. Afterward, the real time NMR assay was started by collecting a set of HSQC spectra along the time course of phosphorylation at 15 °C. For phosphorylation by PLK2, PLK2 (0.75 μg) and the protein (100 μM) were incubated in a Shigemi tube in the NMR spectrometer at 32 °C for 5 min. To obtain efficient phosphorylation and at the same time improve the spectral quality, NMR spectra were recorded at 15 °C during the real time assay, and between the NMR experiments the temperature was set to 30 °C. The experimental time of each ^{1}H-^{15}N HSQC was 56 min. NMR data were processed using Bruker Topspin 1.3 (Bruker Biospin 2005) and NMRPipe (51). The degree of phosphorylation was determined by calculating the intensity of the cross-peak of Ser(P)-129 divided by the sum of the intensities of the phosphorylated and unphosphorylated Ser-129 signal. Error bars were estimated on the basis of the signal-to-noise-ratio in the NMR spectra.

Cell Culture and Transfection—HEK293T and HeLa cells were grown at 37 °C with 5% CO_2 in Dulbecco's modified Eagle's medium (DMEM, GIBCO) supplemented with 10% fetal bovine serum (FBS, GIBCO) and 1% penicillin/streptomycin. For the endogenous phosphorylation studies, 60–80% confluent HEK293T cells in 6-well plates were transiently transfected with 4 μg of pCDNA6.1 to express human α-syn WT and each of the PD-linked mutants, employing the standard calcium phosphate ($CaPO_4$) transfection method. For immunocytochemistry, HeLa cells were seeded on coverslips (12 mm, Milian) that had been precoated with poly-L-lysine (Sigma), for 30 min at room temperature. The cells were transfected with 0.8 μg of each plasmid using Lipofectamine™ 2000 (Invitrogen) according to the manufacturer's instructions. For proteasome activity, cells were co-transfected with 0.5 μg of GFP-CL1 and 3 μg of either of the WT or PD mutants for 72 h. In both cases, the cells were maintained at 37 °C and analyzed 48 h after transfection (unless indicated otherwise).

Cell Lysis and Protein Extraction—Cells were harvested and lysed with 100–150 μl of lysis buffer/well (20 mM Trizma base, 150 mM NaCl, 1 mM EDTA, 0.25% Nonidet P-40, 0.25% Triton-X, pH 7.4) supplemented with 1 mM PMSF (Sigma) and 1:200 protease inhibitor mixture (Sigma). The lysates were vortexed and then kept on ice for 30 min with occasional vortexing. The lysates were then centrifuged at 20,817 × *g* for 15 min at 4 °C. The total amount of protein in the supernatant was estimated with the BCA™ protein assay kit from Thermo Scientific, according to the manufacturer's instructions.

Subcellular Fractionation—The fractionation of HEK293T cells transfected as described above was carried out employing the subcellular proteome extraction kit (Calbiochem catalog no. 539790) according to the manufacturer's instructions. Buffers were also enriched with phosphatase inhibitors (2 mM $NaVO_3$; 5 mM NaF and okadaic acid) to block rapid dephosphorylation. The fractions were immediately analyzed by Western blotting, and their purity was further evaluated by control antibodies (as specified above) against subcellular markers of cell compartments, such as cytosol, membrane/particulate, and nucleus (anti-Hsp90, anti-calnexin, and anti-PARP-1, respectively).

Isolation of ER Microsomes—HEK293T cells were cultured and transfected as described above. ER-microsome extraction was performed using the endoplasmic reticulum enrichment kit (IMGENEX, catalog no. 10088K). Briefly, 36×10^6 cells were washed twice with ice-cold 1× PBS and resuspended with 1 ml of 1× isosmotic homogenization buffer enriched with protease inhibitors. The cells were transferred into a glass Dounce homogenizer (Fisher brand) and homogenized with 12 strokes. The soluble fraction of the homogenate was obtained by centrifugation at 1000 × *g* for 10 min at 4 °C, and the pellet containing nuclei and cell debris was discarded. The resulting supernatant was further centrifuged at 12,000 × *g* for 15 min at 4 °C, and the soluble fraction (free of mitochondria and cell debris) was carefully transferred to a clean microcentrifuge tube for ER isolation. The ER-microsome fraction was obtained by centrifugation of 600 μl of the supernatant at 90,000 × *g* for 1 h at 4 °C and was analyzed as described below.

Gel Electrophoresis (SDS-PAGE) and Immunoblotting—Lysates adjusted to equal amounts of total protein were diluted in loading buffer and separated on 15% SDS 1.5-mm gels. The proteins were then transferred to a nitrocellulose membrane using the TRANS-BLOT SEMI-DRY transfer cell (Bio-Rad) for 45 min at room temperature. The nitrocellulose membrane was blocked with Odyssey blocking buffer (Li-COR Biosciences GmbH) diluted 1:3 in PBS (Sigma) for 1 h at room temperature.

The membrane was probed with the primary antibody and incubated at 4 °C overnight. After four washes in PBST (PBS 0.01% (v/v) Tween 20 (Fluka)), the membrane was incubated with the secondary antibody (*i.e.* goat anti-mouse Alexa Fluor 680) with protection from light at room temperature for 1 h. The immunoblot was finally washed four times with PBST and three times with PBS and scanned using a Li-COR scanner at a wavelength of 700 nm. The band intensity of Ser(P)-129 α-syn obtained on the membrane after Western blot was estimated using ImageJ software and normalized against the signal of total α-syn of the same sample on the same blot. The experiments were repeated six times with the same pattern of results. Statistical analysis was performed using the one-way ANOVA, Scheffe test.

Yeast cells were lysed in Tris-HCl buffer, pH 7.4, with glass beads, in the presence of protease and phosphatase inhibitor mixture (Roche Applied Science). Immunoblotting was performed following standard procedures. Proteins were transferred to a nitrocellulose membrane using a Trans-Blot Turbo transfer system (Bio-Rad). One membrane was probed with anti-α-syn, and the other with anti-Ser(P)-129, at 4 °C overnight, to avoid stripping procedures. The membranes were cut at different sizes and hybridized with the different antibodies for α-syn or Ser(P)-129-α-syn, GAPDH (used as loading control), or kinases (Ck2a, GRK2/5, PLK1/2/3/4-Myc). The band intensity of Ser(P)-129 and total α-syn obtained were estimated using ImageJ software and normalized against the corresponding GAPDH signal. Finally, Ser(P)-129 α-syn levels were determined by determining the ratio between both values: (Ser(P)-129/GAPDH)/(α-syn/GAPDH) and normalized to the control (mean ± S.D.). The experiments were repeated at least five times with the same pattern of result. Statistical analysis was performed using the Mann-Whitney test or the Kruskal-Wallis one-way ANOVA test (indicated in the figure legends).

Immunocytochemistry of Mammalian Cell Lines—Immunocytochemistry was performed on HELA cells 48 h post-transfection (described above). Briefly, the cells were washed twice in PBS, incubated with 200 μl of 4% paraformaldehyde for 10 min at room temperature, and then permeabilized with 0.1% Triton X-100 in PBS for 10 min at room temperature. After three washes with washing buffer (0.1% BSA, 0.1% saponin in 1× PBS), nonspecific binding was blocked with 300 μl of 1% BSA in 1× PBS for 30 min. The primary antibody, sheep anti-α-syn 1:500 (AB5336P, Millipore), was mixed with mouse anti-Ser(P)-129 α-syn 1:800 (Wako) and incubated for 1 h at room temperature. The coverslips were washed three times with washing buffer and incubated with donkey anti-mouse Alexa Fluor® 568 (1:1000) and donkey anti-sheep Alexa Fluor® 488 (1:500) secondary antibodies for 1 h at room temperature. After three washes, the cells were stained with 4,6-diamidino-2-phenylindole (DAPI) (200 μl/well) for 5 min at room temperature. The coverslips were mounted on glass slides with 1,4-diazabicyclo2.2.2octane mounting medium and imaged with a Leica SP2 inverted confocal microscope in sequential mode.

Intracerebral Injections of Lentiviral Vectors—Six-month-old male wild-type C57/Bl6 mice were injected with 3 μl of the lentiviral preparations (2.5×10^7 transducing units) into the hippocampus (using a 5-μl Hamilton syringe) as described previously (49). Briefly, mice were anesthetized, placed on a Koft stereotaxic apparatus, and injected in the hippocampus using the following coordinates (hippocampus, anteroposterior −2.0 mm, lateral 1.5 mm, depth 1.3 mm, and cortex, anteroposterior and cortex 0.5 mm, lateral 1.5 mm, depth 1.0 mm), determined as per the Franklin and Paxinos Atlas. The lentiviral vectors were delivered using a Hamilton syringe connected to a hydraulic system to inject the solution at a rate of 1 μl every 2 min. To allow diffusion of the solution into the brain tissue, the needle was left for an additional 5 min after the completion of the injection. Mice received unilateral injections (right side) to allow comparisons against the contralateral side, with LV-control ($n = 8$), LV-WT α-syn ($n = 8$), and LV-E46K α-syn ($n = 8$). Mice were 6 months old at the time of the injection and survived for 1 month after the lentivirus injection. Following guidelines from the National Institutes of Health for the humane treatment of animals, mice were anesthetized with chloral hydrate and flush-perfused transcardially with 0.9% saline. Brains were post-fixed in phosphate-buffered 4% paraformaldehyde, pH 7.4, at 4 °C for 48 h for neuropathological analysis.

Immunohistochemical Analyses of Brain Sections—Analysis of α-syn accumulation was performed in serially sectioned, free-floating, blind-coded vibratome sections from mice injected with LV-control, LV-WT α-syn, and LV-E46K α-syn. Sections were incubated overnight at 4 °C with an anti-α-syn antibody and the Ser(P)-129 α-syn antibody (Wako) and detected by reaction with diaminobenzidine to reveal α-synuclein immunoreactive cells. To verify that α-syn co-localized to neurons, double labeling studies were performed as described previously (49). Blind-coded, 40-μm thick vibratome sections from mouse brains fixed in 4% paraformaldehyde were immunolabeled with the mouse monoclonal antibody against microtubule-associated protein-2, (MAP2, dendritic marker, Millipore). After overnight incubation with the primary antibodies, sections were incubated with FITC to detect MAP2 and Tyramide Signal Amplification™-Direct (Red) system (PerkinElmer Life Sciences) for α-syn, transferred to Super-Frost slides (Fisher Scientific), and mounted under glass coverslips with anti-fading media (Vector Laboratories). All sections were processed simultaneously under the same conditions, and experiments were performed twice. Sections were imaged with a Zeiss ×63 (N.A. 1.4) objective on an Axiovert 35 microscope (Zeiss) with an attached MRC1024 LSCM system (Bio-Rad) (49). For each mouse, a total of three sections were analyzed, and for each section, four fields in the frontal cortex and hippocampus were examined.

Biochemical Analysis of Brain Homogenates—Frozen brain tissue was placed in cold PDGF buffer (1 mM HEPES, 5 mM benzamidine, 2 mM 2-mercaptoethanol, 3 mM EDTA, 0.5 mM magnesium sulfate, 0.05% sodium azide, pH 8.8) comprising phosphatase and protease inhibitors and then homogenized for 1 min on ice. After clearing lysates by centrifugation at 5000 × *g* for 5 min at 4 °C, supernatants were centrifuged at 100,000 × *g* for 1 h at 4 °C. Protein concentrations of resulting supernatants were determined using the BCA™ protein assay kit from Thermo Scientific, and equal protein amounts were heated for 10 min at 70 °C and then separated by gel electrophoresis on

4–12% BisTris SDS-polyacrylamide gels (Invitrogen). After transferring proteins to nitrocellulose membranes using wet transfer system (Bio-Rad), immunoblots were blocked for 1 h with 10% bovine serum albumin (BSA) in PBS and then incubated overnight at 4 °C with primary antibodies. Membranes were then processed using a chemiluminescence kit (Western Lightning Chemiluminescence Reagent Plus; PerkinElmer Life Sciences) and imaged using a VersaDoc system (Bio-Rad).

RESULTS

The E46K Mutant Exhibits Enhanced Ser-129 Phosphorylation in Mammalian Cell Lines and in Yeast—Previous studies have shown that α-syn is constitutively phosphorylated predominantly at Ser-129, and, to a lesser extent at Ser-87 in mammalian cells (52) and *in vivo* (50, 53, 54). To investigate the effect of the PD-linked mutations on α-syn phosphorylation at these two residues, we overexpressed WT α-syn or the PD mutants (A30P, E46K, or A53T) in HEK293T, HeLa, and M17 cells, and assessed α-syn phosphorylation by endogenous kinases 48 post-transfection. Interestingly, using an antibody against Ser(P)-129, we observed that the PD mutants showed a different pattern of Ser(P)-129 phosphorylation compared with WT α-syn. In contrast to a reduction in Ser(P)-129 levels of the A30P mutant, the A53T and E46K mutants exhibited significant enhancement of Ser(P)-129 levels in all three tested cell lines, without affecting total levels of α-syn (Fig. 1*A*, *C,* and *E*). Notably, the extent of phosphorylation for the E46K mutant was consistently much higher and statistically significant compared to A53T by densitometric analysis (two-way ANOVA, $p < 0.05$) (Fig. 1, *B*, *D,* and *F*). In contrast, none of the mutations affected α-syn phosphorylation levels at Ser-87 (Fig. 1, *G* and *H*).

To assess whether the E46K mutant shows enhanced Ser-129 phosphorylation in another cellular model of PD, WT α-syn and the PD-linked mutants (A30P, E46K, and A53T) were expressed in yeast cells under the regulation of an inducible promoter (*GAL1*), and then Ser-129 levels were evaluated by Western blotting. In line with our mammalian cell culture results, the E46K mutant displayed significantly higher Ser(P)-129 levels compared with WT α-syn or the other PD mutants after induction, without affecting the total levels of α-syn (Fig. 1, *I* and *J*). However, the A30P and A53T mutants exhibited similar Ser(P)-129 levels compared with WT α-syn. These findings show that the PD-linked mutations have different effects on Ser-129 α-syn phosphorylation in mammalian cell lines and in yeast.

Kinetics of α-Syn Phosphorylation by PLK2 and CK1—To investigate the molecular mechanisms underlying the increase in Ser(P)-129 levels of the E46K mutant, we first sought to determine whether this increase is due to this mutant being a better substrate for one of α-syn's natural kinases. To do this, we employed heteronuclear NMR spectroscopy on ^{15}N-labeled recombinant α-syn (WT, A30P, E46K, or A53T) after incubating with PLK2, the most efficient kinase known to phosphorylate α-syn specifically at the Ser-129 residue (43, 55, 56). This method allows the identification of phosphorylation sites, measures the level of integration, and yields kinetic data for the enzymatic modification of individual sites (57). To obtain single-residue resolution and identify all potential phosphorylation sites, the enzymatic reaction was followed by two-dimensional ^{1}H-^{15}N heteronuclear correlation spectra. For all proteins, the resonances were sharp and showed limited dispersion of chemical shifts, reflecting a high degree of backbone mobility (Fig. 2*A*). Phosphorylated serine and threonine residues were readily detected and reflected by phosphorylation shifts of their amide proton resonance downfield of ~8.8 ppm, to an empty region of the ^{1}H-^{15}N HSQC spectrum (Fig. 2*A*). With increasing incubation time, the intensity of the NMR signal of Ser(P)-129 increased with a concomitant decrease of unphosphorylated Ser-129. In agreement with our previous data from cell culture assays (43), only Ser-129 was phosphorylated, highlighting the specificity of PLK2 for Ser-129 phosphorylation. Quantitative analysis of the phosphorylation kinetics of all four proteins was implemented based on the measurement of resonance intensity. After 1 day, 40–50% of the WT protein and of the three α-syn mutants was phosphorylated at Ser-129, and the reaction reached saturation in the following 10 h (Fig. 2*B*). Interestingly, comparing the kinetics of phosphorylation revealed that WT α-syn was phosphorylated faster than all three genetic variants under controlled *in vitro* conditions and using the same kinase and protein concentrations (Fig. 2*B*). Although the saturation levels are only slightly different, the degree of Ser-129 phosphorylation of WT α-syn after 4 h of incubation was larger by a factor of 1.5 when compared with the genetic mutants, hence ruling out the possibility of any of the PD mutants being better substrates for PLK2 *in vitro*.

To assess the kinetics of α-syn phosphorylation at Ser-87, we employed recombinant CK1 enzyme known to phosphorylate α-syn both at Ser-87 and Ser-129 (42), because enzymes phosphorylating specifically at Ser-87 remain unidentified. The NMR signals appearing in the downfield region of the HSQC spectrum were assigned to phosphorylated Ser-87 and phosphorylated Ser-129, confirming that CK1 is capable of phosphorylating both the WT protein and the three genetic variants at these two sites (Fig. 2*C*). Interestingly, and in line with our findings with PLK2, although the rate of phosphorylation of all three mutants and WT α-syn was nearly identical at Ser-87 (Fig. 2*D*), WT α-syn showed again a slightly higher rate of phosphorylation at Ser-129 (Fig. 2*E*). It is worth noting that the similar phosphorylation kinetics of all four proteins at Ser-87 served as a ruler and established that the conditions of the phosphorylation reaction were identical.

The E46K Mutant Is Not a Better Substrate for α-syn's Kinases in Yeast and Mammalian Cell Lines and Does Not Affect Endogenous Kinase Levels—To establish whether the increase in E46K-associated Ser(P)-129 levels is due to the mutant being a better substrate for serine kinases in living cells, we evaluated whether a selected group of kinases that are known to phosphorylate α-syn at Ser(P)-129 is able to specifically increase Ser(P)-129 levels of the E46K mutant in cell-based assays. As such, WT or E46K α-syn were first co-expressed with GRK2, GRK5, CK2, and PLK1/2/3/4 in a yeast model of PD, and the levels of Ser(P)-129 were determined by immunoblotting 5 h after the induction of α-syn overexpression. Fig. 3, *A–C,* shows that co-expression of WT or E46K α-syn with GRK5, PLK2, or PLK3 resulted in a significant increase of Ser(P)-129 levels that was similar for

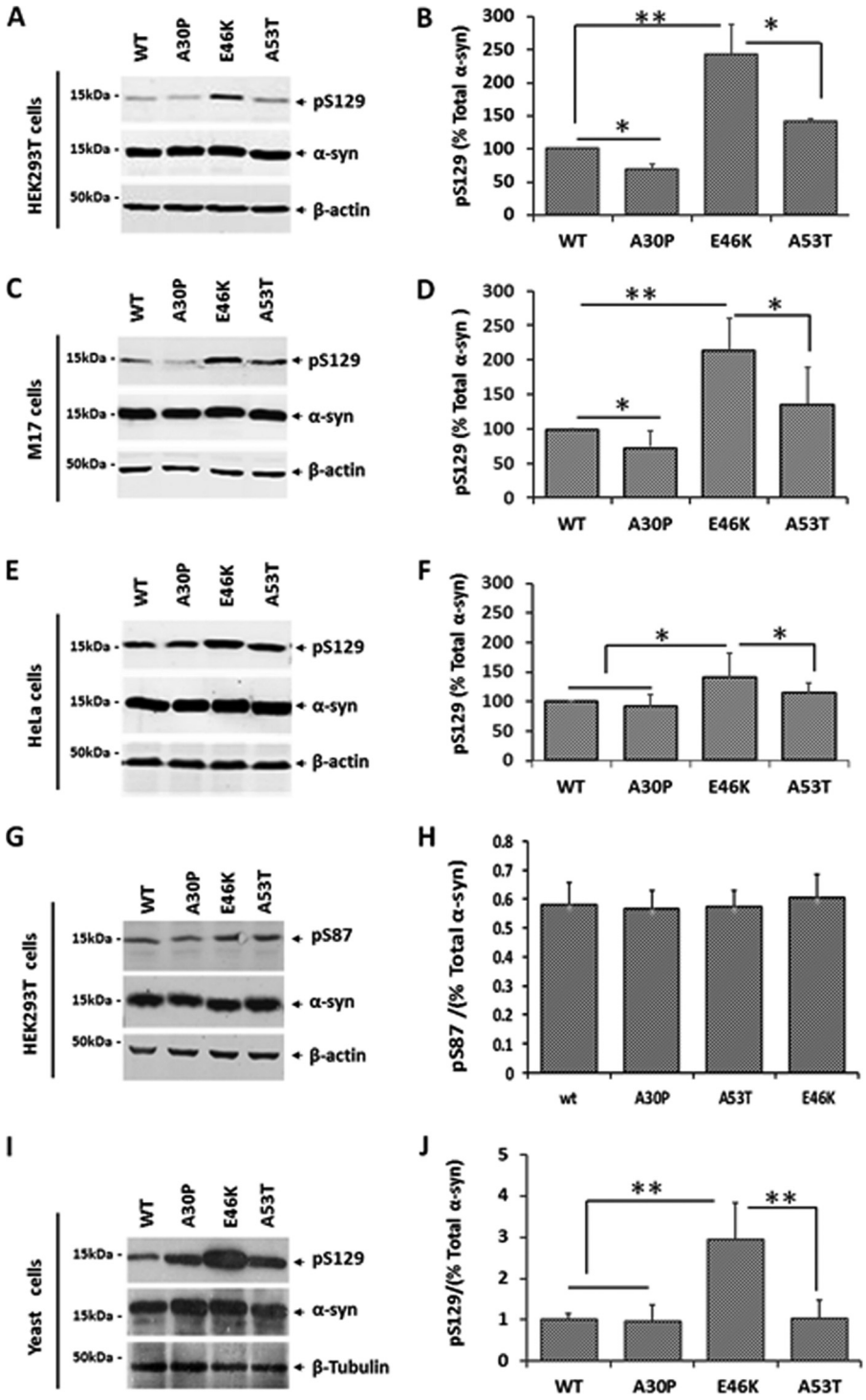

FIGURE 1. **The E46K mutant exhibits enhanced phosphorylation at Ser-129 in mammalian cell lines.** HEK293T, M17, or HeLa cells were transiently transfected with WT or PD mutant α-syn and analyzed by Western blotting 48 h later. Representative Western blots showing total and Ser(P)-129 protein levels in HEK293T (*A*), M17 (*C*), and HeLa (*E*) cells. β-Actin denotes equal protein loading. The E46K α-syn mutant exhibits a significant increase in Ser(P)-129 levels compared with WT α-syn or the A30P and A53T mutants, as assessed by densitometric analysis of Ser(P)-129 levels against total α-syn in HEK293T (*B*), M17 (*D*), and HeLa (*F*) cells. *G*, Western blot showing total protein levels and phosphorylation at Ser-87 in HEK cells. *H*, no significant differences in Ser(P)-87 levels were observed by densitometric analysis. *I*, representative Western blot showing levels of total protein expression and endogenous phosphorylation of α-syn at Ser-129 in yeast 5 h post-α-syn expression induction with galactose. β-Actin was used to normalize protein loading. *J*, increased phosphorylation observed with the E46K mutant was assessed by densitometry analysis of Ser(P)-129 signal against total α-syn (Kruskal-Wallis one-way ANOVA test: **, p value < 0.01; *, $p < 0.5$). The figure is representative of five independent experiments.

both α-syn variants tested (Fig. 3, *A*–*C*). Importantly, the same result was obtained upon co-expression of α-syn (WT or PD mutant) with PLK2 (Fig. 4, *A* and *B*) in mammalian HEK293T cells, hence ruling out the possibility of the E46K mutant being a better substrate for these tested kinases in yeast or mammalian cells. As shown in Fig. 4, *A* and *B*, the overex-

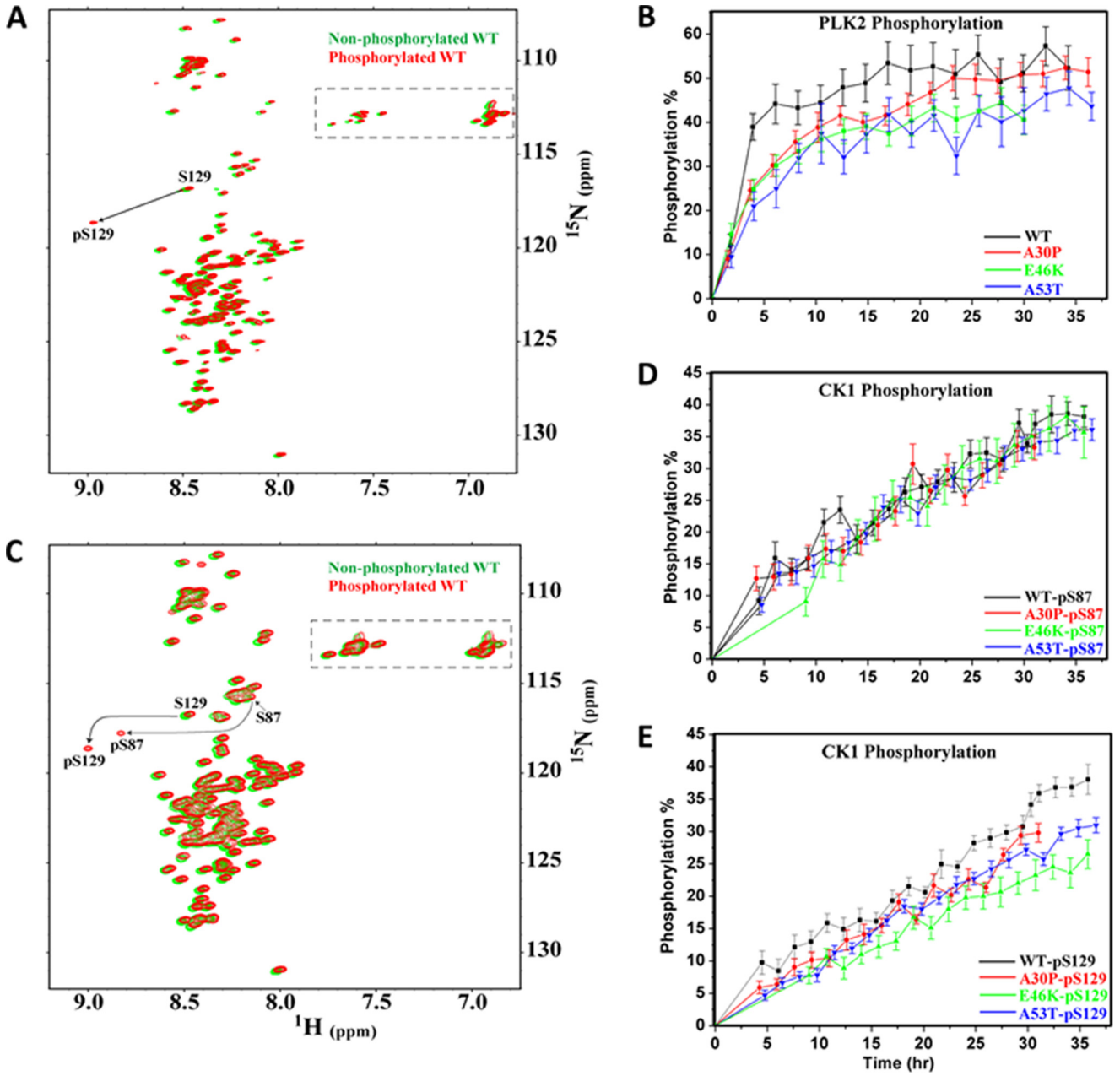

FIGURE 2. **Kinetics of WT and PD-mutant α-syn phosphorylation by PLK2 and CK1.** *A,* comparison of two-dimensional ^{1}H-^{15}N HSQC spectra of unphosphorylated WT (*green*) and PLK2-phosphorylated WT α-syn at Ser-129 (*red*). A *dashed rectangle* marks glutamine and asparagine side chain resonances. *B,* kinetics of *in vitro* phosphorylation of WT (*black*), A30P (*red*), E46K (*green*), and A53T (*blue*) α-syn by PLK2 at Ser-129. The reactions were monitored by real time NMR spectroscopy. *C,* comparison of two-dimensional ^{1}H-^{15}N HSQC spectra of unphosphorylated WT (*green*) and CKI-phosphorylated α-syn at Ser-129 and Ser-87 (*red*). Kinetics of *in vitro* phosphorylation by CKI at Ser-87 (*D*) and Ser-129 (*E*) of WT (*black*), A30P (*red*), E46K (*green*), and A53T (*blue*) α-syn. The reactions were monitored by real time NMR spectroscopy. *Error bars* are based on the signal/noise ratio observed in the NMR spectra.

pression of PLK2 masked the difference in Ser-129 phosphorylation among WT α-syn and all the PD mutants, including E46K.

Next, we investigated whether the increase in Ser(P)-129 levels of the E46K mutant is due to an increase in the levels of endogenous kinases in response to overexpression of the E46K mutant mammalian cells. As such, we evaluated the expression levels of seven α-syn kinases (CK1α, GRK2, GRK3, GRK5, GRK6, PLK2, and PLK3) known to phosphorylate α-syn in cell lines (43, 58, 59). Notably, we did not observe significant changes in expression level of any of these kinases after the overexpression of WT α-syn or any of the PD mutants, as revealed by Western blotting and densitometric quantification (Fig. 4, *C* and *D*).

Enhanced Phosphorylation Observed with the E46K Mutant Is Not Linked with Differential Alteration of α-syn Proteasomal Degradation—Given that phosphorylated α-syn at Ser-129 has been shown to be preferentially cleared via the proteasomal pathway (60, 61), we sought to determine whether the increase in E46K Ser(P)-129 levels is due to this mutant being less efficiently degraded by the proteasome compared to WT α-syn. Therefore, we assessed the effect of inhibiting proteasomal degradation using the potent inhibitor MG132 on E46K Ser(P)-129 levels. As a positive control, we monitored the level of HSP70,

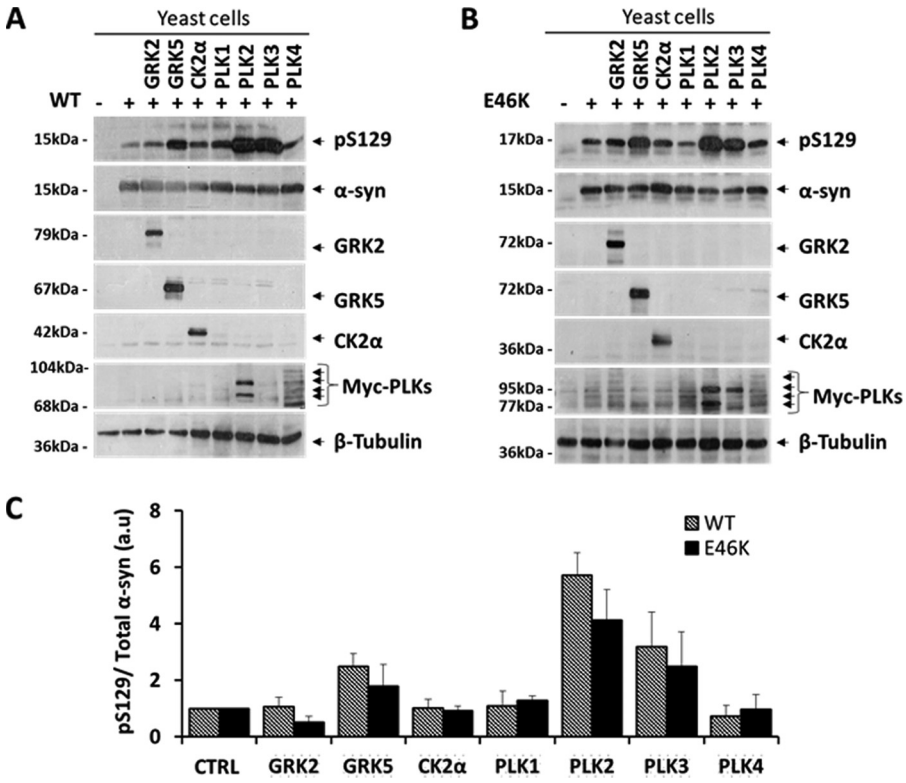

FIGURE 3. **Phosphorylation of WT and E46K α-syn by exogenous kinases in yeast.** Western blot showing total protein levels and phosphorylation at Ser-129 of WT α-syn (*A*) or E46K α-syn (*B*) when expressed either alone or with the indicated human kinases after 5 h of α-syn expression induction with galactose. *C*, densitometric quantification showing significant increase of Ser(P)-129 levels of WT α-syn and E46K α-syn when co-expressed with GRK5, PLK2, or PLK3 in yeast cells (Mann-Whitney test: **, $p < 0.01$; *, $p < 0.5$). The figure is representative of five independent experiments.

which is known to accumulate when proteasomal activity is impaired (62, 63). Fig. 5*A* shows that treatment with MG132 resulted in the accumulation of HSP70. Moreover, and as reported previously (60, 61), MG132 treatment significantly enhanced Ser(P)-129 levels of WT α-syn and all three PD mutants without affecting their total levels (Fig. 5, *A* and *B*). Nevertheless, E46K α-syn consistently showed increased Ser-129 phosphorylation, suggesting that the increased levels are not due to the mutant being less readily degraded by the proteasome and that an additional factor induced by the E46K mutant contributes to the observed accumulation of Ser(P)-129.

To determine whether the E46K mutant inhibits the proteasome activity *per se* more than the other mutants, we co-overexpressed α-syn (WT or PD mutants) with GFP-CL1, a reporter protein that is known to be exclusively degraded by the proteasomal pathway and hence serves as a marker for proteasomal impairment (64, 65). Interestingly, although all three mutants showed significant accumulation of GFP-CL1 compared with WT α-syn, both the A53T and E46K mutants consistently exhibited higher levels of GFP-CL1 (Fig. 5, *C* and *D*). This suggests that all three PD mutants inhibit the proteosomal degradation pathway, albeit to different levels, and that the enhanced Ser(P)-129 levels observed with the E46K mutant are not directly linked with differential inhibition of proteasomal activity.

The E46K Mutant Shows Enhanced Nuclear and ER Accumulation in HEK293T and HeLa Cell Lines—To determine whether the increase in E46K α-syn phosphorylation is due to changes in the subcellular localization of this mutant, we first assessed the subcellular distribution of WT α-syn and the PD-linked mutants by biochemical fractionation. HEK293T cells expressing WT α-syn or PD mutants were lysed, and the cell homogenates were separated into three purified fractions (cytosolic, membrane, and nuclear) and analyzed by Western blotting. Probing for housekeeping proteins, HSP90, calnexin, and PARP1a (which are cytosolic, membrane, and nuclear specific proteins, respectively) allowed determination of fraction purity. Strikingly, although WT and mutant forms of α-syn showed similar abundance in cytosolic fractions (Fig. 6, *A* and *D*), the E46K mutant consistently showed prominent accumulation in nuclear fractions (Fig. 6, *B* and *E*) and slight enrichment in membrane fractions (Fig. 6, *C* and *F*), compared with WT α-syn and the other PD mutants. In contrast, and in line with previous reports, the A30P mutant exhibited a slight decrease in membrane localization (24). Notably, although Ser(P)-129 immunoreactivity was detected in purified cytosolic and membrane fractions (with the E46K mutant consistently exhibiting the highest levels) (Fig. 6, *A* and *C*), it was always below detection limits in nuclear fractions (Fig. 6*B*). Dot blot analysis, however, revealed an increase of Ser(P)-129 immunoreactivity in nuclear fractions of cells expressing WT and PD mutants compared with nontransfected cells (Fig. 6*G*), suggesting that phosphorylated α-syn in the nucleus could be modified (*i.e.* C- or N-terminally truncated as suggested previously (66, 67)) and hence difficult to detect by conventional denaturing gel electrophoresis. The specificity of Ser(P)-129 detection was validated by the transfection of HEK cells with S129A α-syn, a

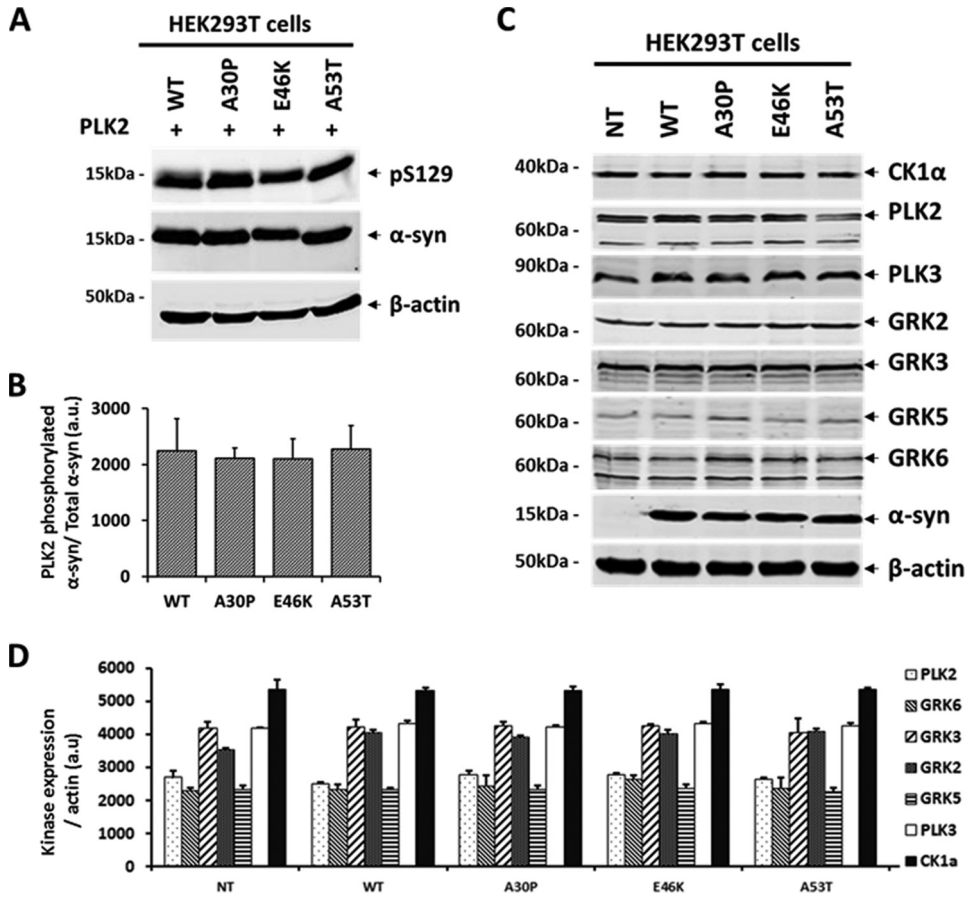

FIGURE 4. **E46K mutant is not a preferential substrate for PLK2 and does not affect endogenous levels of α-syn kinases in HEK293T cells.** *A,* Western blot shows that the extent of α-syn phosphorylation upon co-overexpression with PLK2 is similar for WT α-syn and the PD mutants 24 h post-transfection. *B,* densitometric analysis of Ser(P)-129 signals normalized against the total levels of α-syn. No significant differences were observed with any of the PD mutants compared with WT α-syn when co-expressed with PLK2 (one-way ANOVA test, $n = 3$). *C,* expression levels of endogenous α-syn kinases was assessed in HEK293T cells transiently transfected with WT or mutant α-syn as shown by representative Western blots. *D,* densitometric analysis of Western blots shown reveals no significant differences in kinase protein levels upon overexpression of WT α-syn or any of the PD mutants (one-way ANOVA test, $n = 3$). *a.u.,* arbitrary unit.

mutant obtained by substitution of serine (–OH) with alanine (–CH3) at position 129, hence blocking phosphorylation (Fig. 6*G*). The fact that the signal obtained with the cells overexpressing this mutant did not differ from that of nontransfected cells confirms that anti-Ser(P)-129 α-syn antibody shows superior reactivity with genuinely phosphorylated Ser(P)-129 α-syn.

To confirm the subcellular localization of the E46K mutant, immunocytochemistry was performed on HeLa cells expressing either WT or E46K α-syn using an antibody raised against the C-terminal domain of α-syn (118–131; SA-3400). Importantly, E46K α-syn-expressing cells consistently showed more nuclear α-syn staining compared with cells expressing the WT protein (Fig. 6*H*, *upper panel*), thus confirming our biochemical fractionation data. Moreover, staining using the Ser(P)-129-specific antibody (WAKO) showed that cells expressing WT α-syn exhibit mostly nuclear localization of Ser(P)-129. Significantly more E46K α-syn-expressing cells exhibit perinuclear accumulation of Ser(P)-129 (30%) (Fig. 6*H*, *middle panel*). The specificity of Ser(P)-129 detection was again validated by the transfection of HeLa cells with the S129A mutant of α-syn, which showed weak background staining (Fig. 6*H*, *lower panel*).

Recent studies have shown that Ser(P)-129 α-syn accumulates within the ER/microsomes of symptomatic α-syn transgenic mouse brains and human post-mortem tissues, where it could form toxic oligomeric species at disease onset (68). Therefore, we sought to determine whether the increased perinuclear accumulation of Ser(P)-129 E46K could be associated with the ER, by assessing the co-localization of DsRed-ER (a red fluorescent protein containing the calreticulin ER targeting signal and an ER retention sequence) with WT or PD α-syn mutants in HeLa cells. Interestingly, immunocytochemical analysis showed that the E46K mutant exhibits prominent perinuclear co-localization of Ser(P)-129 with Dsred-ER, suggesting that phosphorylated E46K could be accumulating in the ER (Fig. 6*H*). Moreover, biochemical extraction of ER/microsomes from cells expressing α-syn WT and PD mutants showed increased accumulation of the E46K mutant in ER fractions (Fig. 6*I*), although similar levels of all proteins were detected in the crude and cytosolic fractions. In line with our findings and previous studies showing very low levels of Ser(P)-129 in organelles (*i.e.* nuclei, microsomes) (68–70), we failed to detect Ser(P)-129 in microsomal fractions by Western blotting (Fig. 6*I*). However, analyzing fractionated lysates by dot blots revealed increased Ser(P)-129 levels of all three mutants and WT α-syn compared with nontransfected cells (Fig. 6*J*), hence suggesting that its levels are too low, or that additional modifi-

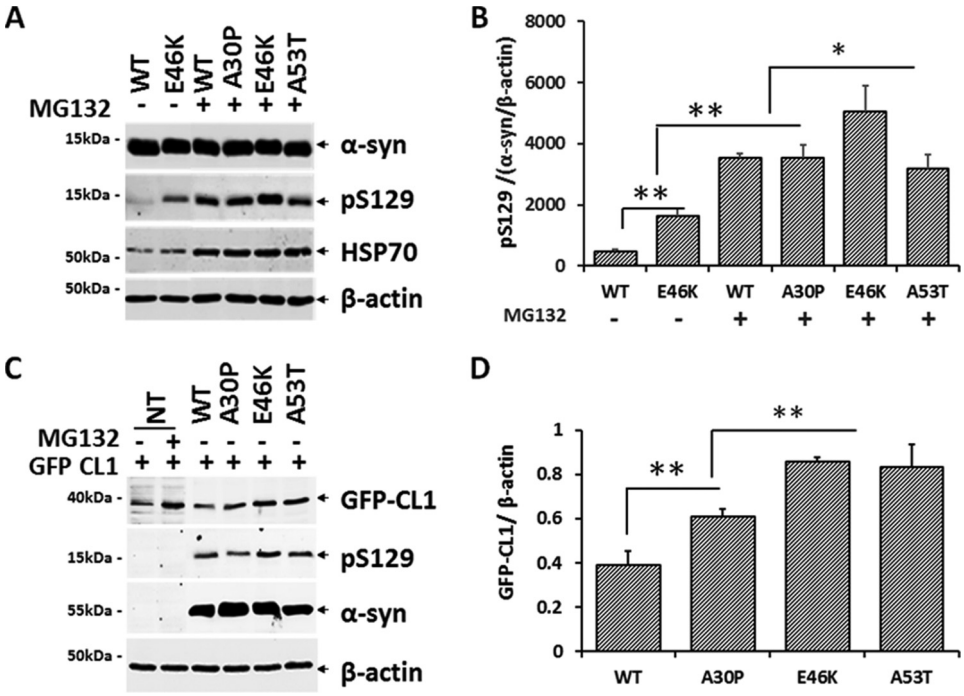

FIGURE 5. **Effect of the E46K mutant on the activity of proteasome-mediated degradation in HEK293T cells.** *A,* MG132 does not reverse the enhanced phosphorylation of the E46K mutant observed in nontreated cells, but it significantly enhances the level of Ser(P)-129 compared to basal levels in the absence of inhibitor. Accumulation of the proteasomally degraded HSP70 protein was used to control for MG132 inhibition. *B,* quantification of Ser(P)-129 levels in the presence of MG132. The E46K mutant shows highest Ser(P)-129 levels compared to WT α-syn and other mutants with/without MG132 treatment. *C,* effect of PD mutants on proteasomal activity. α-syn and PD mutants were co-transfected with a proteasomally degraded protein GFP Degron (GFP-CL1) for 72 h. Representative Western blots indicating the accumulation of GFP-CL1 in response to the overexpression of WT α-syn and its PD-linked mutants. *D,* quantification of GFP-CL1 signal normalized against β-actin indicates significant impairment of proteasomal activity by A30P and much higher inhibition by E46K and A53T.

cations (such as truncation) or interaction with other proteins or cellular compartments/organelles may be hindering its detection by Western blotting.

Enhanced Phosphorylation of the E46K Mutant in the Hippocampus of Lentivirally Injected Mouse Brains—Having demonstrated that the E46K mutation provokes enhanced phosphorylation at Ser-129 in mammalian cell lines and in yeast, we investigated whether similar enhanced E46K α-syn phosphorylation could be observed *in vivo*. We expressed α-syn WT or the E46K mutant in the hippocampus of adult mice using a lentiviral delivery system, and we assessed Ser(P)-129 levels by immunohistochemistry and biochemical analyses. As controls, a group of mice were injected with lentiviruses encoding an empty vector. One month post-injection, sections from mice overexpressing WT or E46K α-syn showed diffuse immunoreactivity to the antibody specific for α-syn (Millipore) throughout cell bodies and neurites (Fig. 7*A*, *middle* and *lower panels*). This contrasts with the staining of control mice where endogenous α-syn showed a much weaker signal that was predominantly punctate reflecting its presynaptic localization in the brain (Fig. 7*A*, *upper panel*). Importantly, Ser(P)-129 staining demonstrated positive reactivity within the cell soma that was more intense in E46K-expressing neurons compared to those expressing WT α-syn (Fig. 7*A*). Neuronal expression of both proteins was confirmed by immunofluorescent co-staining with the neuronal specific marker MAP2 (Fig. 7, *B* and *C*), which again revealed stronger Ser(P)-129 staining for E46K α-syn (Fig. 7*C*), despite the fact that the immunoreactivity for total α-syn was similar for both proteins (Fig. 7*B*). To assess quantitatively the extent of α-syn phosphorylation at Ser-129, brain extracts of mice injected with empty vector, WT α-syn, or the E46K mutant were resolved on SDS-polyacrylamide gels and probed with total and Ser(P)-129-specific antibodies. In line with our immunohistochemistry data, and our data from mammalian cells and yeast, Western blotting and densitometric analysis revealed >2-fold increase in Ser(P)-129 levels in animals injected with lentiviruses encoding E46K compared with WT α-syn (Fig. 7, *D–F*), although similar levels of total α-syn expression were detected (Fig. 7, *D* and *E*). Altogether, these findings demonstrate that the E46K mutant exhibits enhanced phosphorylation at Ser-129 *in vivo*.

DISCUSSION

The E46K Mutant Exhibits an Increase in Ser(P)-129 α-syn Levels—Despite the abundant accumulation of Ser(P)-129 in LBs, the molecular mechanism regulating this process remains poorly understood. In the attempt to unravel factors affecting Ser-129 phosphorylation and aggregation, we set out to investigate the effect of three PD-linked mutations (A30P, E46K, and A53T) on Ser-129 and Ser-87 phosphorylation side-by-side. Interestingly, the E46K mutant showed most pronounced Ser(P)-129 phosphorylation in several tested mammalian cell lines, without affecting phosphorylation at Ser-87. Importantly, this finding was confirmed in another cellular model using yeast overexpressing WT α-syn and PD-linked mutations, as well as in mouse brains in *vivo*. Our results are consistent with previous studies reporting that not only WT but also A30P and A53T mutants are constitutively phosphorylated at the

Ser-129 residue when transiently overexpressed in neuroblastoma SHSY5Y cells (40). Moreover, our finding that both E46K and A53T mutants exhibit enhanced phosphorylation, albeit to different extents, is in line with a recent study by Emmer *et al.* (39) showing that α-syn from transgenic mice expressing either of these mutants is hyperphosphorylated at Ser-129 compared with α-syn from mice expressing the WT protein (39).

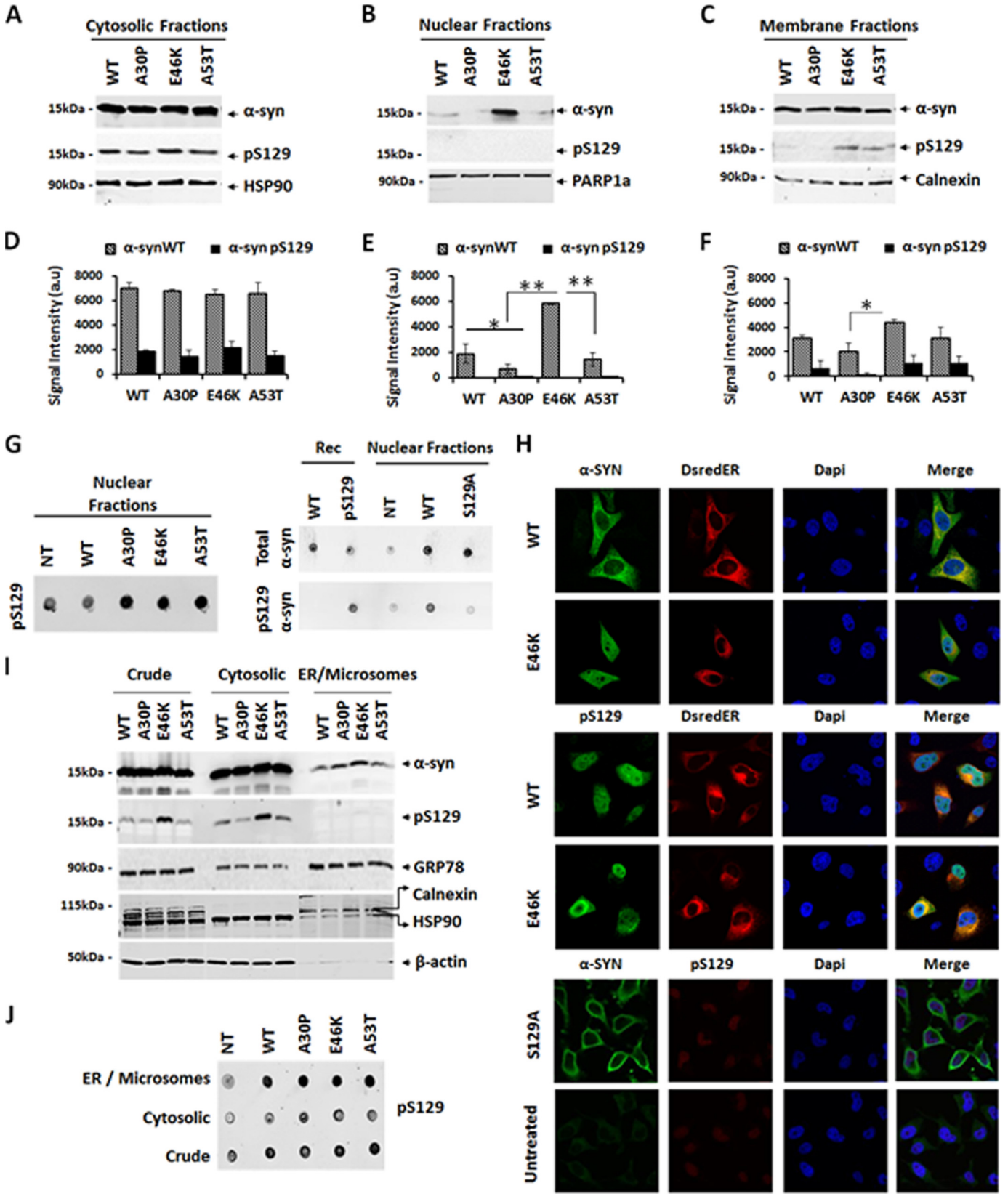

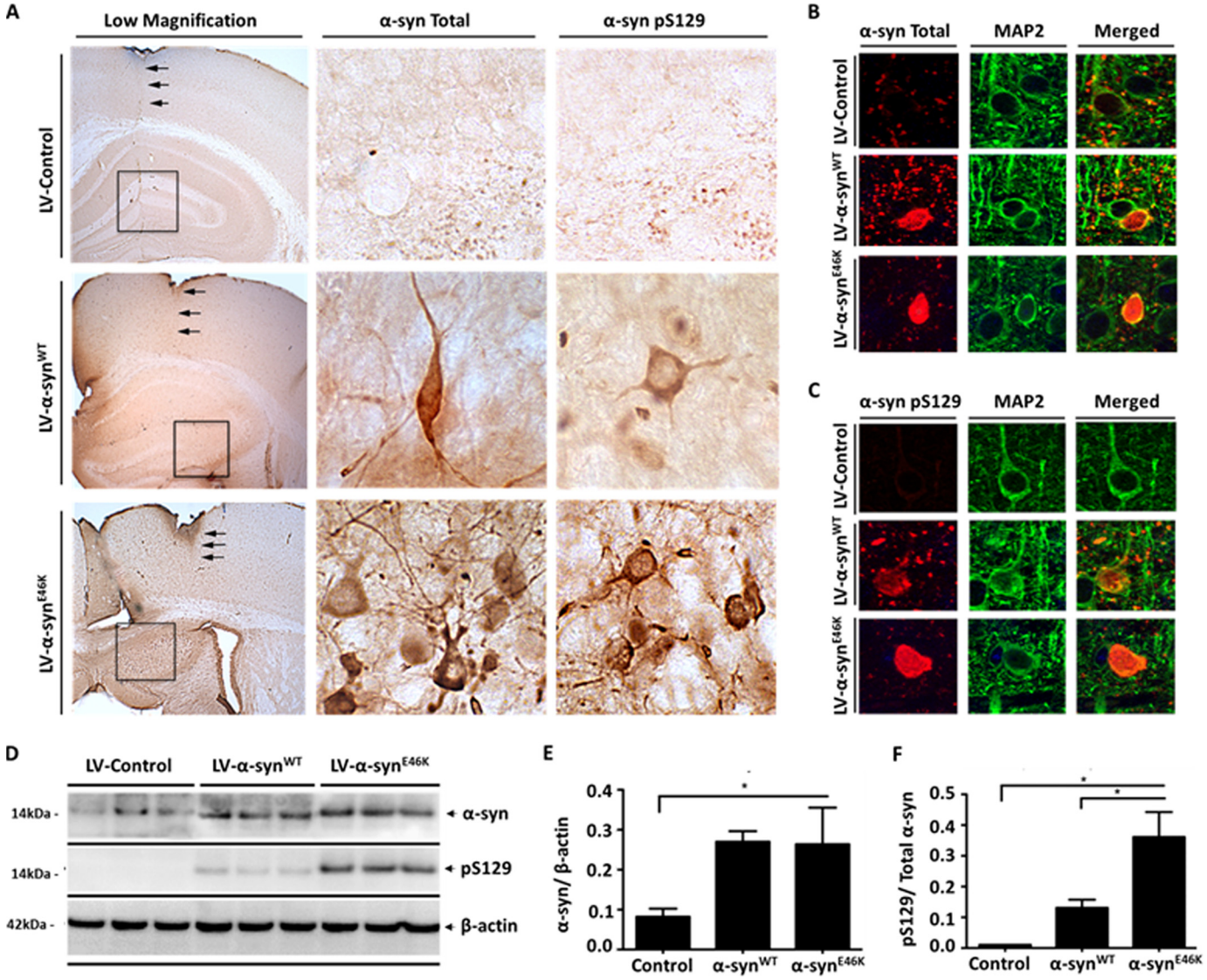

FIGURE 7. **E46K α-syn mutant exhibits enhanced phosphorylation in the hippocampus of lentivirally injected mice.** *A,* immunohistochemical analysis of hippocampal sections of mice injected with LV-control (*top panel*), LV-α-syn^{WT} and LV-α-syn^{E46K} (*middle* and *bottom panels,* respectively) verifies expression and phosphorylation of both proteins in neuronal soma and processes. *B* and *C,* α-syn and Ser(P)-129 immunoreactivities were neuronal specific as they co-localize with MAP2 staining in this brain region. *D–F,* Western blot and densitometric analysis of mice brain homogenates shows significant increased Ser-129 phosphorylation in mice expressing LV-α-syn^{E46K} compared with LV-control and LV-WT ($n = 3$), although similar levels of total proteins were noted in the same fractions.

Given that the E46K mutation only affected phosphorylation at Ser-129 and not at Ser-87 in our assays, we hypothesized that the E46K mutation could alter the structural features of the C-terminal domain of α-syn in ways that make it more susceptible to phosphorylation by kinases. To test this hypothesis, we evaluated the effect of the E46K mutation on α-syn phosphorylation at Tyr-125, another C-terminal phosphorylation site that has been detected in familial cases of PD (71). Strikingly,

FIGURE 6. **The E46K mutation alters the subcellular localization of α-syn.** *A–C,* representative Western blots showing the proportion of WT and mutant α-syn in cytosolic (*A*), nuclear (*B*), and membrane (*C*) fractions. Whereas WT α-syn and PD mutants were predominantly and similarly detectable in cytosolic fractions (*A* and *D*), the E46K mutant showed slightly increased accumulation in membrane fractions (*C* and *F*), and significant enrichment in nuclear fractions (*B* and *E*). Ser(P)-129 in contrast was predominantly enriched in cytosolic fractions (*A* and *D*), barely detectable in membrane fractions (*C* and *F*), and no Ser(P)-129 signal was observed in nuclear fractions (*B* and *E*). *Error bars* represent the average of four independent experiments ($n = 4$). *G,* dot blot analysis showing the immunoreactivity against the Ser(P)-129 antibody in the nuclear fractions of HEK cells overexpressing WT or PD mutant α-syn (*left panel*). The *right panel* shows a separate dot blot experiment validating the specificity of the anti-Ser(P)-129 α-syn antibody, as it selectively detected PLK3-phosphorylated recombinant (*rec*) α-syn at Ser(P)-129 and transfected WT α-syn in nuclear fractions, and not recombinant WT α-syn or the nonphosphorylatable S129A α-syn mutant. *NT* denotes nontransfected cells. *H,* E46K accumulates within the ER. Immunolabeling of total (*upper panel*) and Ser(P)-129 (*middle panel*) α-syn *versus* DsRed ER in HeLa cells shows co-localization of both proteins in cells co-overexpressing DsRed ER and E46K α-syn. *Lower panel,* double immunolabeling using antibodies specific to total α-syn (Biomol) and Ser(P)-129 (Wako) shows that the S129A mutant blocks α-syn phosphorylation at that specific residue. Nuclei were counterstained with DAPI. *I,* subcellular fractionation of HEK293T cells expressing WT and all PD mutants shows significant accumulation of E46K in ER/microsomal fractions. Probing with antibodies against ER proteins (GRP78 and calnexin) and cytosolic proteins (HSP90 and actin) was performed to establish fraction enrichment and purity. *J,* dot blot analysis of ER/microsomal fractions of cells expressing α-syn and PD mutants. Immunoreactivity against Ser(P)-129 antibody was obtained with cells expressing α-syn and PD mutants, and less with nontransfected cells.

the E46K mutation also significantly enhanced phosphorylation at Tyr-125 (data not shown), thereby suggesting that the E46K mutation could be altering the structure of the C terminus of α-syn or its interaction with the N-terminal region of the protein in ways that lead to enhanced phosphorylation at serine or tyrosine residues in this region.

The E46K Mutant Is Not a Better Substrate for Kinases in Vitro, in Cell Lines, and in Yeast and Does Not Modulate the Expression of Endogenous Kinases—Intrigued by the enhanced phosphorylation of the E46K mutant at Ser-129, we asked whether it could also be due to this mutant being a better substrate for a natural α-syn kinase. To address this question, we first evaluated the extent of *in vitro* phosphorylation of the α-syn PD mutants by the following two kinases that are known to phosphorylate α-syn efficiently at Ser-129 and Ser-87 using real time NMR: PLK2 (phosphorylating at Ser-129) and CK1 (phosphorylating at Ser-129 and Ser-87). Our results show that α-syn WT and the PD mutants exhibit similar phosphorylation levels at Ser-129 and Ser-87, with slightly faster kinetics for the WT protein at Ser-129. These findings are consistent with previous reports showing slower *in vitro* phosphorylation of A30P and A53T compared with WT α-syn by CK2 (41). This suggests that the observed E46K-associated hyper-phosphorylation in cell lines and in yeast could be mediated by other kinases or catalyzed by intracellular co-factors. Accordingly, we tested whether a selected group of human kinases described to phosphorylate α-syn at Ser-129 (CK1, CK2, PLK1, PLK2, PLK3, GRK2, GRK3, GRK5, and GRK6) is able to specifically increase Ser(P)-129 levels of the E46K mutant in cellular assays. Importantly, none of these kinases showed preferential phosphorylation of any of the PD mutants in mammalian cells and in yeast. It is worth noting, however, that boosting the kinase levels by transient overexpression might lead to saturated conditions where subtle differences may not be easily discerned.

Next, we asked whether the increase in Ser(P)-129 levels of the E46K mutant is due to the mutant up-regulating the levels of one (or more) endogenous kinases in mammalian cells. Interestingly, none of the screened kinases showed any significant changes in expression levels, hence suggesting that the increase in E46K Ser(P)-129 levels is not mediated via direct up-regulation of any of these endogenous kinases.

Overexpression of the E46K Mutant Does Not Differentially Affect α-syn Proteasomal Degradation in HEK293T Cells—Using MG132 and lactacystin, two small molecular inhibitors of proteasome degradation, Machiya *et al.* (61) demonstrated that phosphorylated α-syn at Ser-129 is preferentially degraded via the proteasome in a ubiquitin-independent manner. Similar results were also reported when employing epoxomycin as a proteasome inhibitor (60). Although several groups have investigated the effect of PD-linked mutations on proteosomal inhibition (65, 72–75), a side-by-side comparison of all three mutants was not performed in any of these studies. Therefore, we assessed the effect of inhibiting proteasomal activity on Ser(P)-129 accumulation of WT α-syn *versus* all three PD-linked mutants. Consistent with previous studies (61), our results showed that inhibition of the proteasome with MG132 significantly elevated the level of phosphorylated WT and PD mutant α-syn. Interestingly, although phosphorylated WT, A30P, and A53T α-syn accumulated to the same level, Ser(P)-129 levels of the E46K mutant remained much higher, suggesting that the increased Ser(P)-129 levels of E46K α-syn are not due to the mutant being less degraded by the proteasome as the proteasome inhibitor did not reverse this effect. Given that WT α-syn and PD mutants were shown to inhibit the proteasome and chaperon-mediated autophagy pathways (65, 72–74, 76), we then tested whether the enhanced Ser(P)-129 accumulation observed with the E46K mutant is conversely due to pronounced proteasomal inhibition by this mutant. Interestingly, both the A53T and E46K mutants exhibited higher proteasomal inhibition compared with WT α-syn as shown previously (72–74, 77). Given that the E46K mutant exhibited significantly higher Ser(P)-129 levels than A53T α-syn, this suggests that the prominent increase in E46K Ser(P)-129 levels is not simply due to proteasomal inhibition alone, which was similar for both mutants.

The E46K Mutant Shows Increased Nuclear Accumulation in Mammalian Cell Lines—Next, we investigated whether the increased E46K phosphorylation could be due to altered subcellular localization of the protein. Strikingly, the E46K mutant showed pronounced nuclear accumulation by biochemical fractionation and immunocytochemical analysis that was accompanied by perinuclear accumulation of Ser(P)-129. Notably, Ser(P)-129 immunoreactivity was always under the limit of detection in nuclear fractions analyzed by Western blotting. Despite several attempts to improve the fractionation and isolation protocols, nuclear Ser(P)-129 could only be detected biochemically by dot blot. These data suggest that either phosphorylation in the nucleus is highly unstable or exists only in trace amounts. It is noteworthy that Ser(P)-129 α-syn has only been reported in the nucleus by immunocytochemical approaches and not by biochemical fractionation and Western blotting (69, 78, 79). One possible explanation of not being able to detect Ser(P)-129 α-syn in the nuclear fractions by these techniques could be due to truncations that might occur under stress conditions and lead to the accumulation of short fragments that can still be phosphorylated at Ser-129 (66). In fact, it has been suggested that this could be the case, where H_2O_2 treatment was shown to induce the translocation of a 10-kDa C-terminal α-syn fragment into the nuclei of dopaminergic cells, while the full-length protein remained sequestered in the cytoplasm (66, 67). As such, the nuclear Ser(P)-129 α-syn signal may actually represent a truncated variant of the protein that can be easily detected by immunofluorescence and dot blot but is too small to be detected biochemically using standard SDS electrophoresis separating techniques.

Nevertheless, when assessing the extent of Ser(P)-129 in the nucleus by dot blot, we failed to detect any differences between the mutants and WT α-syn, despite the higher signal obtained compared with control nontransfected cells. This discrepancy could result from the extraction process and/or from low nonspecific signals that may be observed by dot blot. In fact, sequence alignment of the epitope spanning the Ser(P)-129 region revealed partial homology with a number of nuclear resident proteins (data not shown) that could also be also slightly contributing to the observed Ser(P)-129 signal by dot blot, thus masking subtle differences in Ser(P)-129 levels between the E46K mutant and the other α-syn variants.

E46K α-syn is Sequestered within the Endoplasmic Reticulum—Given that Ser(P)-129 α-syn has been shown to accumulate within the ER/microsomes of α-syn transgenic mouse brains and in human post-mortem tissues (68), we investigated whether the increased perinuclear accumulation of Ser(P)-129 E46K α-syn actually associates with the ER. Interestingly, immunocytochemical analysis revealed strong co-localization between Ser(P)-129 E46K α-syn and Dsred-ER (an ER marker), and biochemical analysis of ER fractions showed pronounced enrichment of the E46K mutant in ER/microsome fractions compared with WT α-syn, hence suggesting that phosphorylated E46K could be accumulating in the ER. Moreover, although Ser-129-phosphorylated α-syn was under our limit of detection by Western blotting in ER-enriched fractions, dot blot analysis showed strong immunoreactivity of Ser-129-phosphorylated α-syn in ER samples obtained from cells expressing α-syn but not control nontransfected cells, suggesting that overexpressing α-syn significantly enhances Ser(P)-129 immunoreactivity in the ER and that other post-translational modifications (such as truncation) might be also occurring in the ER (as suggested with nuclear Ser(P)-129). Our observation that only total E46K is enriched in the cellular organelles such as nucleus and ER might suggest that Ser-129 phosphorylation could be regulating the subcellular localization of the protein, by attenuating its transport from these organelles. Conversely, it could also be that the E46K mutation *per se* leads to aberrant localization of α-syn, which in turn leads to enhanced Ser(P)-129 levels. Further studies are needed to unravel which of these possibilities is indeed taking place.

In summary, we showed that the E46K mutant exhibits enhanced Ser-129 phosphorylation in mammalian cell lines, yeast, as well as in mouse brains compared with WT α-syn and other mutants. The increased Ser(P)-129 E46K levels were not mediated by enhanced phosphorylation of E46K by a specific kinase *in vitro*, in yeast, or in mammalian cell lines nor due to the up-regulation of endogenous levels of expressed kinases. However, our data suggest that the increase in E46K phosphorylation could be linked with enriched nuclear and ER accumulation of E46K α-syn. These findings suggest that the different PD-linked mutations may contribute to the pathogenesis of PD via different mechanisms. Therefore, a side-by-side analysis of transgenic models overexpressing the WT α-syn and the E46K mutant may provide novel insights into the mechanisms underlying the preferential increase of E46K phosphorylation at Ser-129, as well as the interplay between PD mutations and pathogenic post-translational modifications.

Acknowledgments—We thank Nathalie Jordan and John Perrin for technical assistance and Olga Sin for cloning of GRK2, GRK5, and CK2 in the yeast expression vectors. p426TEF CK2α was kindly provided by Dr. Iris Dotan (Tel Aviv University). Bovine GRK2 and GRK5 were kindly provided by Dr. Richard Premont (Duke University).

REFERENCES

1. Oueslati, A., Fournier, M., and Lashuel, H. A. (2010) Role of post-translational modifications in modulating the structure, function and toxicity of α-synuclein: implications for Parkinson's disease pathogenesis and therapies. *Prog. Brain Res.* **183,** 115–145
2. Golbe, L. I., Di Iorio, G., Bonavita, V., Miller, D. C., and Duvoisin, R. C. (1990) A large kindred with autosomal dominant Parkinson's disease. *Ann. Neurol.* **27,** 276–282
3. Polymeropoulos, M. H., Lavedan, C., Leroy, E., Ide, S. E., Dehejia, A., Dutra, A., Pike, B., Root, H., Rubenstein, J., Boyer, R., Stenroos, E. S., Chandrasekharappa, S., Athanassiadou, A., Papapetropoulos, T., Johnson, W. G., *et al.* (1997) Mutation in the α-synuclein gene identified in families with Parkinson's disease. *Science* **276,** 2045–2047
4. Puschmann, A., Ross, O. A., Vilariño-Güell, C., Lincoln, S. J., Kachergus, J. M., Cobb, S. A., Lindquist, S. G., Nielsen, J. E., Wszolek, Z. K., Farrer, M., Widner, H., van Westen, D., Hägerström, D., Markopoulou, K., Chase, B. A., *et al.* (2009) A Swedish family with *de novo* α-synuclein A53T mutation: evidence for early cortical dysfunction. *Parkinsonism Relat. Disord.* **15,** 627–632
5. Krüger, R., Kuhn, W., Müller, T., Woitalla, D., Graeber, M., Kösel, S., Przuntek, H., Epplen, J. T., Schöls, L., and Riess, O. (1998) Ala30Pro mutation in the gene encoding α-synuclein in Parkinson's disease. *Nat. Genet.* **18,** 106–108
6. Zarranz, J. J., Alegre, J., Gómez-Esteban, J. C., Lezcano, E., Ros, R., Ampuero, I., Vidal, L., Hoenicka, J., Rodriguez, O., Atarés, B., Llorens, V., Gomez Tortosa, E., del Ser, T., Muñoz, D. G., and de Yebenes, J. G. (2004) The new mutation, E46K, of α-synuclein causes Parkinson and Lewy body dementia. *Ann. Neurol.* **55,** 164–173
7. Appel-Cresswell, S., Vilarino-Guell, C., Encarnacion, M., Sherman, H., Yu, I., Shah, B., Weir, D., Thompson, C., Szu-Tu, C., Trinh, J., Aasly, J. O., Rajput, A., Rajput, A. H., Jon Stoessl, A., and Farrer, M. J. (2013) α-Synuclein p.H50Q, a novel pathogenic mutation for Parkinson's disease. *Mov. Disord.* **28,** 811–813
8. Proukakis, C., Dudzik, C. G., Brier, T., MacKay, D. S., Cooper, J. M., Millhauser, G. L., Houlden, H., and Schapira, A. H. (2013) A novel α-synuclein missense mutation in Parkinson disease. *Neurology* **80,** 1062–1064
9. Lesage, S., Anheim, M., Letournel, F., Bousset, L., Honoré, A., Rozas, N., Pieri, L., Madiona, K., Dürr, A., Melki, R., Verny, C., Brice, A., and French Parkinson's Disease Genetics Study Group. (2013) G51D α-Synuclein mutation causes a novel parkinsonian-pyramidal syndrome. *Ann. Neurol.* **73,** 459–471
10. Pasanen, P., Myllykangas, L., Siitonen, M., Raunio, A., Kaakkola, S., Lyytinen, J., Tienari, P. J., Pöyhönen, M., and Paetau, A. (2014) A novel α-synuclein mutation A53E associated with atypical multiple system atrophy and Parkinson's disease-type pathology. *Neurobiol. Aging* **35,** 2180
11. Weinreb, P. H., Zhen, W., Poon, A. W., Conway, K. A., and Lansbury, P. T., Jr. (1996) NACP, a protein implicated in Alzheimer's disease and learning, is natively unfolded. *Biochemistry* **35,** 13709–13715
12. Davidson, W. S., Jonas, A., Clayton, D. F., and George, J. M. (1998) Stabilization of α-synuclein secondary structure upon binding to synthetic membranes. *J. Biol. Chem.* **273,** 9443–9449
13. Bertoncini, C. W., Jung, Y. S., Fernandez, C. O., Hoyer, W., Griesinger, C., Jovin, T. M., and Zweckstetter, M. (2005) Release of long-range tertiary interactions potentiates aggregation of natively unstructured α-synuclein. *Proc. Natl. Acad. Sci. U.S.A.* **102,** 1430–1435
14. Schmid, A. W., Chiappe, D., Pignat, V., Grimminger, V., Hang, I., Moniatte, M., and Lashuel, H. A. (2009) Dissecting the mechanisms of tissue transglutaminase-induced cross-linking of α-synuclein: implications for the pathogenesis of Parkinson disease. *J. Biol. Chem.* **284,** 13128–13142
15. Eliezer, D., Kutluay, E., Bussell, R., Jr., and Browne, G. (2001) Conformational properties of α-synuclein in its free and lipid-associated states. *J. Mol. Biol.* **307,** 1061–1073
16. Iwai, A., Masliah, E., Yoshimoto, M., Ge, N., Flanagan, L., de Silva, H. A., Kittel, A., and Saitoh, T. (1995) The precursor protein of non-A β component of Alzheimer's disease amyloid is a presynaptic protein of the central nervous system. *Neuron* **14,** 467–475
17. Jensen, P. H., Nielsen, M. S., Jakes, R., Dotti, C. G., and Goedert, M. (1998) Binding of α-synuclein to brain vesicles is abolished by familial Parkinson's disease mutation. *J. Biol. Chem.* **273,** 26292–26294
18. Lashuel, H. A., Overk, C. R., Oueslati, A., and Masliah, E. (2013) The many faces of α-synuclein: from structure and toxicity to therapeutic target. *Nat. Rev. Neurosci.* **14,** 38–48
19. Ahn, K. J., Paik, S. R., Chung, K. C., and Kim, J. (2006) Amino acid sequence

motifs and mechanistic features of the membrane translocation of α-synuclein. *J. Neurochem.* **97,** 265–279
20. Ulmer, T. S., Bax, A., Cole, N. B., and Nussbaum, R. L. (2005) Structure and dynamics of micelle-bound human α-synuclein. *J. Biol. Chem.* **280,** 9595–9603
21. Bodner, C. R., Maltsev, A. S., Dobson, C. M., and Bax, A. (2010) Differential phospholipid binding of α-synuclein variants implicated in Parkinson's disease revealed by solution NMR spectroscopy. *Biochemistry* **49,** 862–871
22. Kim, Y. S., Laurine, E., Woods, W., and Lee, S. J. (2006) A novel mechanism of interaction between α-synuclein and biological membranes. *J. Mol. Biol.* **360,** 386–397
23. Bussell, R., Jr., and Eliezer, D. (2004) Effects of Parkinson's disease-linked mutations on the structure of lipid-associated α-synuclein. *Biochemistry* **43,** 4810–4818
24. Jo, E., Fuller, N., Rand, R. P., St George-Hyslop, P., and Fraser, P. E. (2002) Defective membrane interactions of familial Parkinson's disease mutant A30P α-synuclein. *J. Mol. Biol.* **315,** 799–807
25. Fares, M. B., Ait-Bouziad, N., Dikiy, I., Mbefo, M. K., Jovičić, A., Kiely, A., Holton, J. L., Lee, S. J., Gitler, A. D., Eliezer, D., and Lashuel, H. A. (2014) The novel Parkinson's disease linked mutation G51D attenuates *in vitro* aggregation and membrane binding of α-synuclein, and enhances its secretion and nuclear localization in cells. *Hum. Mol. Genet.* **23,** 4491–4509
26. Choi, W., Zibaee, S., Jakes, R., Serpell, L. C., Davletov, B., Crowther, R. A., and Goedert, M. (2004) Mutation E46K increases phospholipid binding and assembly into filaments of human α-synuclein. *FEBS Lett.* **576,** 363–368
27. Perlmutter, J. D., Braun, A. R., and Sachs, J. N. (2009) Curvature dynamics of α-synuclein familial Parkinson disease mutants: molecular simulations of the micelle- and bilayer-bound forms. *J. Biol. Chem.* **284,** 7177–7189
28. El-Agnaf, O. M., Jakes, R., Curran, M. D., and Wallace, A. (1998) Effects of the mutations Ala30 to Pro and Ala53 to Thr on the physical and morphological properties of α-synuclein protein implicated in Parkinson's disease. *FEBS Lett.* **440,** 67–70
29. Conway, K. A., Harper, J. D., and Lansbury, P. T., Jr. (2000) Fibrils formed *in vitro* from α-synuclein and two mutant forms linked to Parkinson's disease are typical amyloid. *Biochemistry* **39,** 2552–2563
30. Narhi, L., Wood, S. J., Steavenson, S., Jiang, Y., Wu, G. M., Anafi, D., Kaufman, S. A., Martin, F., Sitney, K., Denis, P., Louis, J. C., Wypych, J., Biere, A. L., and Citron, M. (1999) Both familial Parkinson's disease mutations accelerate α-synuclein aggregation. *J. Biol. Chem.* **274,** 9843–9846
31. Giasson, B. I., Uryu, K., Trojanowski, J. Q., and Lee, V. M. (1999) Mutant and wild type human α-synucleins assemble into elongated filaments with distinct morphologies *in vitro*. *J. Biol. Chem.* **274,** 7619–7622
32. Greenbaum, E. A., Graves, C. L., Mishizen-Eberz, A. J., Lupoli, M. A., Lynch, D. R., Englander, S. W., Axelsen, P. H., and Giasson, B. I. (2005) The E46K mutation in α-synuclein increases amyloid fibril formation. *J. Biol. Chem.* **280,** 7800–7807
33. Yonetani, M., Nonaka, T., Masuda, M., Inukai, Y., Oikawa, T., Hisanaga, S., and Hasegawa, M. (2009) Conversion of wild-type α-synuclein into mutant-type fibrils and its propagation in the presence of A30P mutant. *J. Biol. Chem.* **284,** 7940–7950
34. Ghosh, D., Mondal, M., Mohite, G. M., Singh, P. K., Ranjan, P., Anoop, A., Ghosh, S., Jha, N. N., Kumar, A., and Maji, S. K. (2013) The Parkinson's disease-associated H50Q mutation accelerates α-synuclein aggregation *in vitro*. *Biochemistry* **52,** 6925–6927
35. Li, J., Uversky, V. N., and Fink, A. L. (2001) Effect of familial Parkinson's disease point mutations A30P and A53T on the structural properties, aggregation, and fibrillation of human α-synuclein. *Biochemistry* **40,** 11604–11613
36. Conway, K. A., Lee, S. J., Rochet, J. C., Ding, T. T., Williamson, R. E., and Lansbury, P. T., Jr. (2000) Acceleration of oligomerization, not fibrillization, is a shared property of both α-synuclein mutations linked to early-onset Parkinson's disease: implications for pathogenesis and therapy. *Proc. Natl. Acad. Sci. U.S.A.* **97,** 571–576
37. Ghosh, D., Sahay, S., Ranjan, P., Salot, S., Mohite, G. M., Singh, P. K., Dwivedi, S., Carvalho, E., Banerjee, R., Kumar, A., and Maji, S. K. (2014) The newly discovered Parkinson's disease associated Finnish mutation (A53E) attenuates α-synuclein aggregation and membrane binding. *Biochemistry* **53,** 6419–6421
38. Anderson, J. P., Walker, D. E., Goldstein, J. M., de Laat, R., Banducci, K., Caccavello, R. J., Barbour, R., Huang, J., Kling, K., Lee, M., Diep, L., Keim, P. S., Shen, X., Chataway, T., Schlossmacher, M. G., *et al.* (2006) Phosphorylation of Ser-129 is the dominant pathological modification of α-synuclein in familial and sporadic Lewy body disease. *J. Biol. Chem.* **281,** 29739–29752
39. Emmer, K. L., Waxman, E. A., Covy, J. P., and Giasson, B. I. (2011) E46K human α-synuclein transgenic mice develop Lewy-like and tau pathology associated with age-dependent, detrimental motor impairment. *J. Biol. Chem.* **286,** 35104–35118
40. Smith, W. W., Margolis, R. L., Li, X., Troncoso, J. C., Lee, M. K., Dawson, V. L., Dawson, T. M., Iwatsubo, T., and Ross, C. A. (2005) α-Synuclein phosphorylation enhances eosinophilic cytoplasmic inclusion formation in SH-SY5Y cells. *J. Neurosci.* **25,** 5544–5552
41. Ishii, A., Nonaka, T., Taniguchi, S., Saito, T., Arai, T., Mann, D., Iwatsubo, T., Hisanaga, S., Goedert, M., and Hasegawa, M. (2007) Casein kinase 2 is the major enzyme in brain that phosphorylates Ser129 of human α-synuclein: implication for α-synucleinopathies. *FEBS Lett.* **581,** 4711–4717
42. Paleologou, K. E., Schmid, A. W., Rospigliosi, C. C., Kim, H. Y., Lamberto, G. R., Fredenburg, R. A., Lansbury, P. T., Jr., Fernandez, C. O., Eliezer, D., Zweckstetter, M., and Lashuel, H. A. (2008) Phosphorylation at Ser-129 but not the phosphomimics S129E/D inhibits the fibrillation of α-synuclein. *J. Biol. Chem.* **283,** 16895–16905
43. Mbefo, M. K., Paleologou, K. E., Boucharaba, A., Oueslati, A., Schell, H., Fournier, M., Olschewski, D., Yin, G., Zweckstetter, M., Masliah, E., Kahle, P. J., Hirling, H., and Lashuel, H. A. (2010) Phosphorylation of synucleins by members of the Polo-like kinase family. *J. Biol. Chem.* **285,** 2807–2822
44. Hoyer, W., Antony, T., Cherny, D., Heim, G., Jovin, T. M., and Subramaniam, V. (2002) Dependence of α-synuclein aggregate morphology on solution conditions. *J. Mol. Biol.* **322,** 383–393
45. Outeiro, T. F., and Lindquist, S. (2003) Yeast cells provide insight into α-synuclein biology and pathobiology. *Science* **302,** 1772–1775
46. Mumberg, D., Müller, R., and Funk, M. (1995) Yeast vectors for the controlled expression of heterologous proteins in different genetic backgrounds. *Gene* **156,** 119–122
47. Premont, R. T. (1994) Identification of adenylyl cyclases by amplification using degenerate primers. *Methods Enzymol.* **238,** 116–127
48. Dotan, I., Ziv, E., Dafni, N., Beckman, J. S., McCann, R. O., Glover, C. V., and Canaani, D. (2001) Functional conservation between the human, nematode, and yeast CK2 cell cycle genes. *Biochem. Biophys. Res. Commun.* **288,** 603–609
49. Spencer, B., Potkar, R., Trejo, M., Rockenstein, E., Patrick, C., Gindi, R., Adame, A., Wyss-Coray, T., and Masliah, E. (2009) Beclin 1 gene transfer activates autophagy and ameliorates the neurodegenerative pathology in α-synuclein models of Parkinson's and Lewy body diseases. *J. Neurosci.* **29,** 13578–13588
50. Paleologou, K. E., Oueslati, A., Shakked, G., Rospigliosi, C. C., Kim, H. Y., Lamberto, G. R., Fernandez, C. O., Schmid, A., Chegini, F., Gai, W. P., Chiappe, D., Moniatte, M., Schneider, B. L., Aebischer, P., Eliezer, D., *et al.* (2010) Phosphorylation at S87 is enhanced in synucleinopathies, inhibits α-synuclein oligomerization, and influences synuclein-membrane interactions. *J. Neurosci.* **30,** 3184–3198
51. Delaglio, F., Grzesiek, S., Vuister, G. W., Zhu, G., Pfeifer, J., and Bax, A. (1995) NMRPipe: a multidimensional spectral processing system based on UNIX pipes. *J. Biomol. NMR* **6,** 277–293
52. Okochi, M., Walter, J., Koyama, A., Nakajo, S., Baba, M., Iwatsubo, T., Meijer, L., Kahle, P. J., and Haass, C. (2000) Constitutive phosphorylation of the Parkinson's disease associated α-synuclein. *J. Biol. Chem.* **275,** 390–397
53. Fujiwara, H., Hasegawa, M., Dohmae, N., Kawashima, A., Masliah, E., Goldberg, M. S., Shen, J., Takio, K., and Iwatsubo, T. (2002) α-Synuclein is phosphorylated in synucleinopathy lesions. *Nat. Cell Biol.* **4,** 160–164
54. Waxman, E. A., and Giasson, B. I. (2008) Specificity and regulation of casein kinase-mediated phosphorylation of α-synuclein. *J. Neuropathol. Exp. Neurol.* **67,** 402–416
55. Inglis, K. J., Chereau, D., Brigham, E. F., Chiou, S. S., Schöbel, S., Frigon,

N. L., Yu, M., Caccavello, R. J., Nelson, S., Motter, R., Wright, S., Chian, D., Santiago, P., Soriano, F., Ramos, C., *et al.* (2009) Polo-like kinase 2 (PLK2) phosphorylates α-synuclein at serine 129 in central nervous system. *J. Biol. Chem.* **284,** 2598–2602

56. Salvi, M., Trashi, E., Marin, O., Negro, A., Sarno, S., and Pinna, L. A. (2012) Superiority of PLK-2 as α-synuclein phosphorylating agent relies on unique specificity determinants. *Biochem. Biophys. Res. Commun.* **418,** 156–160
57. Landrieu, I., Lacosse, L., Leroy, A., Wieruszeski, J. M., Trivelli, X., Sillen, A., Sibille, N., Schwalbe, H., Saxena, K., Langer, T., and Lippens, G. (2006) NMR analysis of a Tau phosphorylation pattern. *J. Am. Chem. Soc.* **128,** 3575–3583
58. Pronin, A. N., Morris, A. J., Surguchov, A., and Benovic, J. L. (2000) Synucleins are a novel class of substrates for G protein-coupled receptor kinases. *J. Biol. Chem.* **275,** 26515–26522
59. Sakamoto, M., Arawaka, S., Hara, S., Sato, H., Cui, C., Machiya, Y., Koyama, S., Wada, M., Kawanami, T., Kurita, K., and Kato, T. (2009) Contribution of endogenous G-protein-coupled receptor kinases to Ser129 phosphorylation of α-synuclein in HEK293 cells. *Biochem. Biophys. Res. Commun.* **384,** 378–382
60. Chau, K. Y., Ching, H. L., Schapira, A. H., and Cooper, J. M. (2009) Relationship between α-synuclein phosphorylation, proteasomal inhibition and cell death: relevance to Parkinson's disease pathogenesis. *J. Neurochem.* **110,** 1005–1013
61. Machiya, Y., Hara, S., Arawaka, S., Fukushima, S., Sato, H., Sakamoto, M., Koyama, S., and Kato, T. (2010) Phosphorylated α-synuclein at Ser-129 is targeted to the proteasome pathway in a ubiquitin-independent manner. *J. Biol. Chem.* **285,** 40732–40744
62. Neznanov, N., Dragunsky, E. M., Chumakov, K. M., Neznanova, L., Wek, R. C., Gudkov, A. V., and Banerjee, A. K. (2008) Different effect of proteasome inhibition on vesicular stomatitis virus and poliovirus replication. *PLoS One* **3,** e1887
63. Boone, A. N., and Vijayan, M. M. (2002) Glucocorticoid-mediated attenuation of the hsp70 response in trout hepatocytes involves the proteasome. *Am. J. Physiol. Regul. Integr. Comp. Physiol.* **283,** R680–R687
64. Gilon, T., Chomsky, O., and Kulka, R. G. (1998) Degradation signals for ubiquitin system proteolysis in *Saccharomyces cerevisiae*. *EMBO J.* **17,** 2759–2766
65. Nonaka, T., and Hasegawa, M. (2009) A cellular model to monitor proteasome dysfunction by α-synuclein. *Biochemistry* **48,** 8014–8022
66. Xu, S., Zhou, M., Yu, S., Cai, Y., Zhang, A., Uéda, K., and Chan, P. (2006) Oxidative stress induces nuclear translocation of C-terminus of α-synuclein in dopaminergic cells. *Biochem. Biophys. Res. Commun.* **342,** 330–335
67. Zhou, M., Xu, S., Mi, J., Uéda, K., and Chan, P. (2013) Nuclear translocation of α-synuclein increases susceptibility of MES23.5 cells to oxidative stress. *Brain Res.* **1500,** 19–27
68. Colla, E., Jensen, P. H., Pletnikova, O., Troncoso, J. C., Glabe, C., and Lee, M. K. (2012) Accumulation of toxic α-synuclein oligomer within endoplasmic reticulum occurs in α-synucleinopathy *in vivo*. *J. Neurosci.* **32,** 3301–3305
69. Wakamatsu, M., Ishii, A., Ukai, Y., Sakagami, J., Iwata, S., Ono, M., Matsumoto, K., Nakamura, A., Tada, N., Kobayashi, K., Iwatsubo, T., and Yoshimoto, M. (2007) Accumulation of phosphorylated α-synuclein in dopaminergic neurons of transgenic mice that express human α-synuclein. *J. Neurosci. Res.* **85,** 1819–1825
70. Colla, E., Coune, P., Liu, Y., Pletnikova, O., Troncoso, J. C., Iwatsubo, T., Schneider, B. L., and Lee, M. K. (2012) Endoplasmic reticulum stress is important for the manifestations of α-synucleinopathy *in vivo*. *J. Neurosci.* **32,** 3306–3320
71. Kiely, A. P., Asi, Y. T., Kara, E., Limousin, P., Ling, H., Lewis, P., Proukakis, C., Quinn, N., Lees, A. J., Hardy, J., Revesz, T., Houlden, H., and Holton, J. L. (2013) α-Synucleinopathy associated with G51D SNCA mutation: a link between Parkinson's disease and multiple system atrophy? *Acta Neuropathol.* **125,** 753–769
72. Jiang, M., Porat-Shliom, Y., Pei, Z., Cheng, Y., Xiang, L., Sommers, K., Li, Q., Gillardon, F., Hengerer, B., Berlinicke, C., Smith, W. W., Zack, D. J., Poirier, M. A., Ross, C. A., and Duan, W. (2010) Baicalein reduces E46K α-synuclein aggregation *in vitro* and protects cells against E46K α-synuclein toxicity in cell models of familiar Parkinsonism. *J. Neurochem.* **114,** 419–429
73. Stefanis, L., Larsen, K. E., Rideout, H. J., Sulzer, D., and Greene, L. A. (2001) Expression of A53T mutant but not wild-type α-synuclein in PC12 cells induces alterations of the ubiquitin-dependent degradation system, loss of dopamine release, and autophagic cell death. *J. Neurosci.* **21,** 9549–9560
74. Tanaka, Y., Engelender, S., Igarashi, S., Rao, R. K., Wanner, T., Tanzi, R. E., Sawa, A., V, L. D., Dawson, T. M., and Ross, C. A. (2001) Inducible expression of mutant α-synuclein decreases proteasome activity and increases sensitivity to mitochondria-dependent apoptosis. *Hum. Mol. Genet.* **10,** 919–926
75. Emmanouilidou, E., Melachroinou, K., Roumeliotis, T., Garbis, S. D., Ntzouni, M., Margaritis, L. H., Stefanis, L., and Vekrellis, K. (2010) Cell-produced α-synuclein is secreted in a calcium-dependent manner by exosomes and impacts neuronal survival. *J. Neurosci.* **30,** 6838–6851
76. Martìn-Clemente, B., Alvarez-Castelao, B., Mayo, I., Sierra, A. B., Dìaz, V., Milán, M., Fariñas, I., Gómez-Isla, T., Ferrer, I., and Castaño, J. G. (2004) α-Synuclein expression levels do not significantly affect proteasome function and expression in mice and stably transfected PC12 cell lines. *J. Biol. Chem.* **279,** 52984–52990
77. McNaught, K. S., and Jenner, P. (2001) Proteasomal function is impaired in substantia nigra in Parkinson's disease. *Neurosci. Lett.* **297,** 191–194
78. Huang, Z., Xu, Z., Wu, Y., and Zhou, Y. (2011) Determining nuclear localization of α-synuclein in mouse brains. *Neuroscience* **199,** 318–332
79. Schell, H., Hasegawa, T., Neumann, M., and Kahle, P. J. (2009) Nuclear and neuritic distribution of serine-129 phosphorylated α-synuclein in transgenic mice. *Neuroscience* **160,** 796–804

Molecular Bases of Disease:

Parkinson Disease Mutant E46K Enhances α-Synuclein Phosphorylation in Mammalian Cell Lines, in Yeast, and *in Vivo*

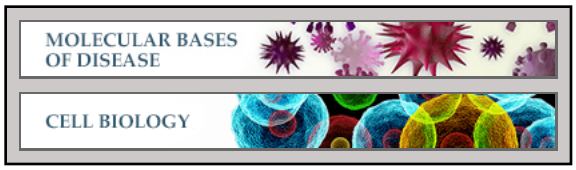

Martial Kamdem Mbefo, Mohamed-Bilal Fares, Katerina Paleologou, Abid Oueslati, Guowei Yin, Sandra Tenreiro, Madalena Pinto, Tiago Outeiro, Markus Zweckstetter, Eliezer Masliah and Hilal A. Lashuel

J. Biol. Chem. 2015, 290:9412-9427.
doi: 10.1074/jbc.M114.610774 originally published online February 5, 2015